VIENNA UNIVERSITY OF TECHNOLOGY
DEPARTMENT OF GEODESY
AND GEOINFORMATION
RESEARCH GROUPS
PHOTOGRAMMETRY & REMOTE SENSING

Master Thesis

Validation of high resolution soil moisture products over Austria

A thesis submitted at the Department of Geodesy and Geoinformation
in fulfillment of the requirements for the degree of Master of Science

under the direction of
Univ.Prof. Dipl.-Ing. Dr.techn. Wolfgang Wagner

and the supervision of
Senior Scientist Dr.techn. Mariette Vreugdenhil

filed at the Vienna University of Technology
Faculty of Mathematics and Geoinformation
by

Dragana Panić

Matriculation number 01228461
Pernerstorfergasse 59/1/10
1100, Vienna

Vienna, April 6th 2020 ....

Declaration

I hereby declare that I have written this thesis by myself without any help or assistance of others. External literature used to clarify the content or provided data sources are fully cited. All mentioned information is in accordance with fact or truth up to my knowledge.

Vienna, April 6th 2020   ....

Abstract

Soil moisture plays an important role in the water, carbon and energy cycle. More and more applications, i.e. in agriculture, climate research, environmental science, need high resolution soil moisture estimates. The objective of this thesis is to validate high resolution soil moisture products over Austria. In this study an existing approach using in situ measurements as control data was extended to a novel approach where groundwater observations are used to evaluate ensemble soil moisture dataset. This work was developed within the BMon project (Bodenfeuchte-Monitoring).

The reference data used in this analysis consists of three in situ soil moisture networks: Hoal, WegenerNet and BMNT. The in situ data was compared against S1ASCAT data, hydrological, meteorological and agrometeorological model datasets as well as the ensemble product. The ensemble product was created by combining S1ASCAT and three model datasets. In this work, the validation for the Hoal SM network was applied at two layer depths, surface soil moisture (SSM) and root zone soil moisture (RZSM), and for the BMNT and WegenerNet SM networks at RZSM. The groundwater measurements, collected from over 2600 sites across Austria, were evaluated against the ensemble product (RZSM), which represents a combination of the individual products that is expected to deliver superior soil moisture estimates.

The pre-processing steps were performed by masking out the data observed in frozen conditions, then using a scaling method to enable valid comparison between soil moisture datasets. After temporal matching between two comparable datasets, the Pearson correlation coefficient and uRMSD were estimated to investigate the relationships between in situ measurements against S1ASCAT and model datasets. In the novel validation approach, the Spearman correlation coefficient between the ensemble dataset and groundwater observations was calculated and the effect of soil porosity and diversity in land cover types on the changes in groundwater table was investigated.

The results show that the quality of high resolution soil moisture products is driven by several parameters which have complex relationships. The most significant factors hereby are precipitation events (as the main source of soil moisture content) as well as soil porosity due to its effect on the soil infiltration rate. The results indicate that the response delays (lags) are found at deeper groundwater layers owing to the slower water infiltration through the soil. High correlations up to 0.8 are found in most cases by comparing ensemble datasets with groundwater measurements, where the groundwater layer depth ranges up to 6 m. When validating the in situ observations of Hoal network, the correlations of R_p up to 0.7 indicate a good agreement with ensemble, S1ASCAT and three model datasets. Slightly lower correlations up to 0.5 are found when comparing with WegenerNet network due to the low number (4) of compared stations because the result can be significantly driven by discrepancies in time series. The BMNT network showed slightly higher correlations with ensemble- and agrometeorological model dataset. The seasonal dependency was estimated by calculating the correlations per season for every in situ network. While positive biases of the satellite observations during the growing

Dragana Panić

season are observed, the capability to record small-scale soil moisture changes from rainfall events is apparent.

Future work should address the effects of soil porosity and heterogeneity in land cover types on soil moisture as well as on groundwater. This finding of a combined product (ensemble) is promising and should be extended by combining many different soil moisture datasets. This study provides the framework for future studies to assess the performance of high resolution Earth Observation data in comparison to in situ measurements and groundwater observations.

Kurzfassung

Bodenfeuchtigkeit spielt eine wichtige Rolle im Wasser-, Kohlenstoff- und Energiekreislauf. Immer mehr Anwendungen, in der Landwirtschaft, Klimaforschung und Umweltwissenschaften, erfordern hochauflösende Bodenfeuchtigkeitsschätzungen. Ziel der Arbeit ist es, hochauflösende Bodenfeuchtigkeitsprodukte über Österreich zu validieren. In dieser Studie wurde ein bestehender Ansatz unter Verwendung von In-situ-Messungen als Kontrolldaten auf einen neuartigen Ansatz erweitert, bei dem Grundwasserbeobachtungen zur Evaluierung des Bodenfeuchtig-keitsdatensatzes des Ensembles verwendet wurden. Diese Arbeit wurde im Rahmen des BMon-Projekts (Bodenfeuchte-Monitoring) entwickelt.

Die in dieser Analyse verwendeten Referenzdaten bestehen aus drei In-situ-Bodenfeuchtigkeitsnetzen: Hoal, WegenerNet und BMNT. Die In-situ-Daten wurden mit S1ASCAT-Daten, hydrologischen, meteorologischen und agrarmeteorologischen Modelldatensätzen sowie dem Ensemble-Produkt verglichen. Das Ensemble-Produkt wurde durch Kombination von S1ASCAT und drei Modelldatensätzen erstellt. In dieser Arbeit wurde die Validierung für das Hoal BF-Netzwerk in zwei Schichttiefen, Oberflächenbodenfeuchte (OBF) und Wurzelzonenbodenfeuchte (WBF), sowie für die BMNT- und WegenerNet BF-Netzwerke in einer Schichttiefe (WBF) angewendet. Die an über 2600 Standorten in ganz Österreich gesammelten Grundwassermessungen wurden gegen des Ensemble-Produkts (WBF) evaluiert, das einzelne Produkte kombiniert und theoretisch genauere Bodenfeuchteschätzungen liefern kann.

Zur Validierung wurden sämtliche Daten unter gefrorenen Bedingungen maskiert und auf einen gemeinsamen Wertebereich skaliert. Nach zeitlichem Abgleich zwischen zwei vergleichbaren Datensätzen wurden der Pearson-Korrelationskoeffizient und uRMSD berechnet, um die Beziehungen zwischen In-situ-Messungen gegen S1ASCAT und Modelldatensätzen zu untersuchen. In dem neuartigen Validierungsansatz zur Bewertung des Ensembles mit Grundwasserbeobachtungen wurde der Spearman-Korrelationskoeffizient berechnet und der Einfluss der Bodenporosität und -diversität in Landbedeckungstypen auf die Änderungen des Grundwasserspiegels untersucht.

Die Ergebnisse der Analyse zeigen, dass die Qualität hochauflösender Bodenfeuchtigkeitsprodukte von mehreren Parametern abhängt, die komplexe Beziehungen aufweisen. Die bedeutendste Rolle bei Veränderungen des Grundwasserspiegels spielen Niederschlagsereignisse (als Hauptquelle für den Bodenfeuchtigkeitsgehalt) sowie die Bodenporosität aufgrund ihrer Auswirkung auf die Bodeninfiltrationsrate. Die Ergebnisse zeigen, dass die Reaktionsverzögerungen in tieferen Grundwasserschichten aufgrund der langsameren Wasserinfiltration durch den Boden auftreten. Hohe Korrelationen bis zu 0,8 werden in den meisten Fällen durch den Vergleich von Ensemble-Datensätzen mit Grundwassermessungen gefunden, bei denen die Grundwasserschichttiefe bis zu 6 m beträgt. Bei der Validierung der In-situ-Beobachtungen des Hoal-Netzwerks zeigen die Korrelationen von R_p bis zu 0,7 die sehr gute Übereinstimmung mit Ensemble, S1ASCAT und den drei Modelldatensätzen. Aufgrund der geringen Anzahl (4) der verglichenen Stationen werden beim Vergleich mit dem WegenerNet-Netzwerk geringfügig geringere Korrelationen

Dragana Panić

von bis zu 0,5 festgestellt, da das Ergebnis erheblich durch Diskrepanzen in Zeitreihen beeinflusst werden kann. Das BMNT-Netzwerk zeigte etwas höhere Korrelationen mit dem Ensemble und dem agrarmeteorologischen Modell. Die saisonale Abhängigkeit wurde geschätzt, indem die Korrelationen pro Saison für jedes In-situ-Netzwerk berechnet wurden. Während positive Verzerrungen der Satellitenbeobachtungen während der Vegetationsperiode beobachtet werden, ist die Fähigkeit, kurzzeitige Bodenfeuchtigkeitsänderungen aufgrund von Niederschlagsereignissen aufzuzeichnen, offensichtlich.

Zukünftige Arbeiten sollten darin bestehen, die Auswirkungen der Bodenporosität und -heterogenität bei Landbedeckungstypen auf die Bodenfeuchtigkeit sowie auf das Grundwasser zu bestimmen. Dieser Befund eines kombinierten Produkts (Ensembles) ist vielversprechend und sollte durch die Kombination vieler verschiedener Bodenfeuchtedatensätze erweitert werden. Diese Studie bietet den Rahmen für zukünftige Studien zur Bewertung der Leistung hochauflösender Erdbeobachtungsdaten im Vergleich zu In-situ-Messungen und Grundwasserbeobachtungen.

Acknowledgements

The present Master Thesis was accomplished at the Department of Geodesy and Geoinformation, Vienna University of Technology. I would like to thank all those who contributed to this research. Special thanks goes to my supervisor Mariette Vreugdenhil, who always had an open ear for my concerns and questions and also motivated me with her expertise and lots of valuable advices. In addition, I want to thank to Prof. Wolfgang Wagner, who gave me the possibility to work in a professional and motivated team and thus offer me the chance to expand my experience in remote sensing.

Many thanks go to my colleague Isabella Pfeil, whose suggestions, discussions and technical assistance were very helpful offering me new perspectives.

I would like to take this opportunity to thank my family for their continuous encouragement and support during my education, especially for always having friendly and understanding ear and time for my concerns as well as for their financial support during my education. I would also like to thank my study colleagues, who accompanied me and encouraged me during my studies. Many thanks go to my salsa friends and my friends from church choir, who shared my passion for dancing and singing and also for offering me a welcome change from a daily routine. It was tremendous! Finally, I want to thank the proofreaders of my thesis, my colleagues and good friends, Tichaona-Tavare Mukunga and Raphael Quast.

Contents

List of Figures

List of Tables

List of Acronyms

AGRO	agrometeorological soil moisture model
ASCAT	Advanced Scatterometer
BMNT	Bundesministerium für Nachhaltigkeit und Tourismus
EO	Earth Observation
ESA CCI	European Space Agency's Climate Change Initiative
HYDRO	hydrological soil moisture model
INCA	Integrated Nowcasting through Comprehensive Analysis
METEO	meteorological soil moisture model
RMSD	Root-Mean-Square Deviation
RZSM	root zone soil moisture
S1ASCAT	combined product of Sentinel-1 and Metop ASCAT product
SM	soil moisture
SSM	surface soil moisture
uRMSD	unbiased Root-Mean-Square Deviation

Dragana Panić

Chapter 1

Introduction

Soil moisture is one of the key variables in the climate system. Dynamics in soil moisture (SM) help us to improve our understanding of many physical, chemical and biological processes on the land surface. Many scientific disciplines use SM datasets for development, estimation and further improvement of their models. The major impact of SM can be recognised in rainfall estimation (Luca Brocca, Massari, et al. 2015), irrigation scheduling (Soulis, Elmaloglou, and Dercas 2015), modelling of groundwater depletion (Rodell, Velicogna, and Famiglietti 2009), drought monitoring (Hao and AghaKouchak 2014; Martínez-Fernández et al. 2016), hydrological model and flood forecasting (Wanders, Bierkens, et al. 2014; Wanders, Karssenberg, et al. 2014) and runoff prediction (Luca Brocca, Melone, et al. 2010). However, many of these studies are tested on models which contain different kinds of errors that are not yet fully investigated and interpreted. Therefore, for any application it is required to use accurate SM observations in order to be able to avoid discrepancies in results that can not be either recognised or corrected later.

The importance of SM as a climatic parameter has risen significantly over the past three decades. It has been recently included in the list of 50 Essential Climate Variables (ECVs) to contribute in further research of the Intergovernmental Panel on Climate Change (IPCC) and United Nations Framework Convention on Climate Change (UNFCCC) (W. Wagner et al. 2012). The first dedicated SM mission Soil Moisture Ocean Salinity (SMOS) (Kerr et al. 2001) was launched in 2009 by the European Space Agency (ESA) which was enhanced in 2015 with a novel dedicated SM mission Soil Moisture Active Passive (SMAP) by NASA (The National Aeronautics and Space Administration)(D. Entekhabi et al. 2008). Both missions utilize L-band and radiometry and measure surface SM fields on a global scale. In spring 2012, the successful follow-up mission of AMSR-E was launched measuring SM retrievals from C-band observations, and it is called the Advanced Microwave Scanning Radiometer 2 (AMSR2) (Robert Parinussa, Holmes, et al. 2015).

The first Meteorological Operational satellite (MetOp-A) was launched in 2006, carry the real aperature radar ASCAT, operating in C-band with vertical polarization. Its application can be found in many research areas, i.e. measuring wind speed and direction over the ocean, monitoring of snow cover, sea- and land- ice as well as SM (Figa-saldaña et al. 2002). Significant interest of evaluating the Advanced Scatterometer (ASCAT) (onboard MetOp-A) estimates over different regions can be found in several studies, i.e. in the Bibeschbach experimental catchment in Luxembourg (Hasenauer 2020), in southwestern France (Clement Albergel et al. 2009),

across three continents (United States of America (USA), Europe and Australia) compared with FLUXNET observational network (Deng et al. 2019), over specific SM networks across Europe (Luca Brocca, Hasenauer, et al. 2011) and in Australia (Holgate et al. 2016). The agreement between satellite SM products and in situ observations has been demonstrated with high correlations validated with robust and standardized approaches. An essential element for this trend investigation is the robustness of quality of observations over time and space (Luca Brocca, Hasenauer, et al. 2011). For example, the results from a study catchment in southwestern France (Clement Albergel et al. 2009) have shown a generally significant correlation level of surface soil moisture (SSM) with slight discrepancies at the soil layer at 5 cm depth due to a shallow (0.5-2 cm) surface soil layer. Deng et al. 2019 presented an approach of analysing the performance of SM product over different land cover type, which has not been successful for comparing ASCAT SM measurements with in situ for needleleaf forests and woody savannas suggesting that the vegetation effects play an important role in sense of consistent SSM estimates. On the other hand, Scott, Bastiaanssen, and Ahmad 2003 have developed an alternative method to derive soil water content, depending on the depth where root water extraction is active. Their study suggested that dynamic behaviour of certain depth occurs with the very dense crops and during the growing vegetation processes.

Another common issue for many research projects besides vegetation effects is a lack of dense in situ SM networks when investigating the spatial and temporal harmony of high resolution SM product with in situ stations. Due to some limitations of the SM sensors like measuring small soil volume, challenges arise when it comes to comparing measurements from single in situ station within a certain area (Crow et al. 2012). Due to soil heterogeneity in satellite footprints, often one in situ SM monitoring station reflects local soil texture or topography. This can result in poor correlation between the two data sources, resulting in the need for additional in situ measurements. This problem of spatio-temporal scales can be reduced but never completely removed. Furthermore, the in situ stations are typically installed outside of agricultural fields which is why their use of SM values to represent the main land use is questionable. Moreover, the microwave SM satellite observations are very sensitive to the soil penetration depth (Schneeberger et al. 2004) due to its strong dependency on the water content, and thus it is difficult to interpret results when the microwave SM observations are compared with in situ SM measurements gained from sensors installed at different depths. This can easily lead to inaccurate results which may not represent the true state.

Much research in recent decades has focused on downscaling global SM products (Merlin et al. 2013, Das et al. 2014, Rüdiger et al. 2016) which simultaneously raised the interest in footprint-scale SM data. In addition, the high resolution radar SM retrievals (Wolfgang Wagner, Sabel, et al. 2010, cek et al. 2012, Gruber et al. 2013) enable global SM monitoring with a long-planned mission lifetime which is why it gives long-lasting and permanent SM values with a nearly-daily global coverage. With these abilities it becomes comparable to different operational missions i.e. MetOp ASCAT. Regarding the MetOp ASCAT which is recording observations with a spatial resolution of 25 km and delivering them on a global scale every 1–3 days, the comparison to the Sentinel-1 (S1) data becomes more attractive. Even though the S1 temporal resolution is still beyond the frequency of meteorological systems, the Synthetic Aperture Radar (SAR) missions are intended to fill this limitation.

However, the validation of high resolution SM is very difficult due to regular comparison with sparse SM networks. In this work, another approach of validating the combined product of very high spatial resolution (100 m) with ground measurements (in situ and groundwater) is proposed.

1.1 Groundwater

In recent years the importance of groundwater recharge attracted much attention due to its influence on the current state of SM. In the hydrology it is still a challenging issue to produce accurate estimations of groundwater recharge. Wang et al. 2016 reported the significant impacts of soil properties and precipitation on groundwater state. Moreover, these authors have evaluated the groundwater recharge using a Hydrus-1D model (Simunek et al. 2008) where the positive matching of simulated SM against groundwater has been found. There still remains a need for an efficient method that can estimate and validate high resolution SM products. An alternative approach for evaluating high resolution satellite SM products using a dense network of groundwater level observations has been developed in Netherlands (Richard de Jeu n.d.). In their analysis they have implemented two 100 m resolution SM datasets (L-band and C-band) and the dense network over a Dutch lowlands. High correlations between AMSR-2 (Advanced Microwave Scanning Radiometer 2) and SMAP (Soil Moisture Active Passive) SM products in comparison to groundwater observations have been observed and better results have been found with the comparison of SMAP observations. Their results have shown better correlations where the shallow groundwater levels occur while descending correlations appear below 150 cm groundwater layer depth. In their study the differences between the seasonal pattern of the SM sensor and the satellite SM product are observed. Furthermore, the groundwater data showed similar seasonal patterns as the satellite SM product and the visible lag of approximately two months between the SM and groundwater is found. In this research the expected lag at the deeper groundwater level will be examined.

Most research studies are dealing with the validation and evaluation of satellite SM products using the correlation coefficients and root mean square differences (Dara Entekhabi et al. 2010, Dorigo et al. 2015, Montzka et al. 2017). Following the suggestions of Colliander et al. 2017, this evaluation was carried out using conventional measures of agreement Pearson correlation and unbiased root mean square difference (ubRMSD) for the comparison with in situ data. The groundwater validation analysis was carried out by calculating the Spearman correlation coefficient, autocorrelation values and standard deviation of differences.

1.2 Objective and Structure of Work

The objective of this research is to validate high resolution SM products from Earth Observation (EO) and models over Austria. In order to assess the quality of high resolution SM products, firstly the validation of ground-based in situ SM measurements was calculated with four SM datasets: S1ASCAT dataset, three model datasets and with its combined product ensemble. Secondly the novel approach of evaluating

groundwater observations in respect to ensemble product over Austria was developed.

The ensemble product was developed within the BMon (Bodenfeuchte-Monitor) project. The objective of the BMon project is to develop a cloud-based system for near-real-time monitoring of SM conditions over Austria at high spatio-temporal resolution (100 m). The ensemble represents the main product of the SM datasets, which combines skills of one S1ASCAT SM product data and three models from hydrology, agronomy and meteorology through model-data integration to obtain high resolution SM estimates. This work will provide the answer on the question is it possible to retrieve high resolution SM estimates by combining S1ASCAT data and model datasets.

Chapter 1 presented a brief introduction about the importance of SM estimates and the current status of different high resolution remote sensing missions to observe SM. Another important part are the studies about the growing interest of validating groundwater observations.

The theoretical background of the validation metrics and statistical parameters used in the analysis will be described in Chapter 2.

An general overview of the study area, which is whole Austria will be covered in Chapter 3. It includes several maps of Austria with average temperature, precipitation, elevation values and different land cover types established from European Space Agency's Climate Change Initiative (ESA CCI) project.

Chapter 4 gives detailed description of the different datasets used in this work. They include S1ASCAT, ensemble and model datasets as well as three in situ networks and one groundwater network. The spatial distribution of three in situ networks and over 2600 groundwater sites across Austria is presented in graphical form.

In addition, this research advances from previous studies of using standard validation metrics as uRMSD, Pearson and Spearman correlation coefficient by implementing the autocorrelation and standard deviation of differences. These methods and its useful performance is briefly explained in Chapter 5.

The Chapter 6 provides the results of two approaches, with the task to validate high resolution SM product in both, space and time. The first approach explores the validation of high resolution SM products, three model datasets and ensemble (as a new downscaled SM product) against in situ SM observations. In second approach a new plan with different methods than have not been used in previous studies was proposed, by testing the hypothesis if there exists a correlation between variations of SM and of the groundwater layer depth.

A detailed discussion on the outcome of the ensemble and if it improve high resolution SM estimates will be presented in Chapter 7. In addition, the effect of different land cover types and which effect it has on the performance of the SM products will be discussed. It sums up challenges of the investigated approaches and relate our results to the findings of previously research analyses.

Finally, the Chapter 7 gives an overall summary, suggestions and an outlook.

Chapter 2

Validation and error characterization

In order to be able to validate and compare different datasets, several statistical parameters as well as commonly used metrics were calculated. The following section briefly describes the statistical parameters that are used often in SM validation to characterize a distribution of continuous random variables. In the section 2.3 the metrics (Pearson and Spearman correlation coefficient) which characterize the agreement or disagreement between two data sets can be found. After applying linear scaling (based on mean and standard deviation (sec. 2.2), the uRMSD was computed which corrects for biases in the mean of the SM fluctuations. Two another metrics, autocorrelation and standard deviation of differences, were used to describe the temporal behavior of time series.

2.1   Statistical parameters

2.1.1   Mean

Mean (or arithmetic mean) of the dataset is the central value of a discrete set of numbers. If the dataset is based on a set of independent observations obtained by sampling (which is the case in this study) the arithmetic mean is referred to the expected value and it is calculated as:

$$\bar{x} = \frac{1}{n}\left(\sum_{i=1}^{n} x_i\right) \tag{2.1}$$

2.1.2   Median

For the dataset, the median can be described as the "middle" value, separating the lower half from the higher half of the data. The median is well known as a robust value in comparison to the mean, which is more sensitive to outliers. It is calculated with following formulas, where need to be distinguished between odd (2.2) or even (2.3) number of observation.

$$md_o = x_{\frac{(n-1)}{2}} \tag{2.2} \qquad\qquad md_e = \frac{1}{2}\left(x_{\frac{n}{2}} + x_{\frac{n}{2}+1}\right) \tag{2.3}$$

2.1.3 Standard deviation

The standard deviation (2.4) is a measure of the amount of variation of a set of values (Altman and Bland 2005). For the case when data represent normal distribution, the 95% of the data are found within two standard deviation of the mean and the other 5% are scattered above or below of the given limit. The standard deviation is the square root of the variance, which represents the spread around its mean.

$$\hat{\sigma_X} = \sqrt{\frac{1}{N} \sum_{i=1}^{N} (x_i - \hat{\mu})^2} \tag{2.4}$$

2.2 Scaling of soil moisture

2.2.1 Mean standard deviation scaling

In this research a mean standard deviation scaling method was applied. This scaling method scales the input datasets so that after the scaling they have the same mean (2.1.1) and standard deviation (2.1.3) as the reference dataset. The formula to apply the mean standard deviation scaling method is:

$$Y^X = \frac{Y - \overline{Y}}{\sigma_Y} \cdot \sigma_X + \overline{X}, \tag{2.5}$$

This scaling method was carried out for the EO, ensemble and three model datasets in respect to the reference in situ measurements.

2.3 Validation metrics

2.3.1 Statistical dependency

2.3.1.1 Linear correlation

Two standard validation metrics are given in Dara Entekhabi et al. 2010 to access the accuracy of remote sensing measurements with respect to true fields. The Pearson correlation coefficient (2.6) is a temporal metric and characterises linear statistical dependency between two datasets and it is given by:

$$\rho_{XY} = \frac{\sigma_{XY}}{\sigma_X \sigma_Y}, \tag{2.6}$$

where the σ_{XY} is a covariance between two datasets X and Y normalized with the standard deviation of the respective dataset $\sigma_X \sigma_Y$. It has a value between -1 and +1, where -1 means the measurements of two datasets build a line with a negative slope, 0 means no linear correlation and +1 means the joint values lie on a line with a positive slope.

2.3.1.2 Rank correlation

Whereas the requirements for the Pearson's correlation are linearity between the paired datasets and their bivariate normally distribution, the Spearman's correlation requires no normality which is why it is a nonparametric statistic. Spearman's rank correlation coefficient (2.7) is a statistical measure of the strength of a monotonic relationship between two variables:

$$\rho_{XY} = \frac{\sigma_{rXrY}}{\sigma_{rX}\sigma_{rY}}. \tag{2.7}$$

The interpretation of temporal Spearman rank correlation coefficients is similar to Pearsons, the closer ρ_{XY} is to the ± 1 the robuster the monotonic relationship between two paired data.

2.3.2 Absolute deviations

2.3.2.1 Unbiased Root Mean Squared Difference (uRMSD)

The third validation metric used in this work is the absolute metric unbiased Root-Mean-Square Deviation (uRMSD) (Los 2009). It is derived from the Root-Mean-Square Deviation (RMSD) (2.8) which is calculated from following formula:

$$\text{RMSD} = \sqrt{\frac{1}{N}\sum_{i=1}^{N}(X_i - Y_i)^2}. \tag{2.8}$$

It is square root of the averaged squared differences between predicted values and observed values. Therefore, the calculated values represent the average absolute deviation between matched measurements. Moreover, the RMSD is formed of different error sources and the effect of each error can influence the total RMSD from minor to the significant intense. In this work, the bias term that comes from additive and multiplicative systematic differences and scaling errors was corrected by subtracting it from the RMSD. The resulting metric is called unbiased RMSD (uRMSD)(2.9), expressed by:

$$\text{uRMSD} = \sqrt{\frac{1}{N}\sum_{i=1}^{N}(X_i - Y_i^X)^2}. \tag{2.9}$$

Equations (2.8) through (2.9) are related throughout following expression:

$$\text{uRSMD}^2 = \text{RMSD}^2 - \text{Bias}^2. \tag{2.10}$$

In comparison to the (2.8) the ubRSMD contains one term with superscript calculating the rescaling between reference dataset Y and some dataset X. Therefore, the value of uRMSD is mainly driven by random errors of the dataset with a high dependency of the trend of the reference dataset.

Chapter 3

Study area

In this research the validation and evaluation was performed over three study areas. First, the groundwater evaluation was carried out over Austria. The characteristics of Austria are described in section 3.1. The in situ SM validation was performed over two core sites, which are the HOAL (sec. 3.2) and the WegenerNet (sec. 3.3) and over whole Austria, where the BMNT stations (sec. 3.4) are distributed.

3.1 Geography of Austria

3.1.1 Climate

The validation of SM has been carried out over whole Austria. As the quantity of SM is affected by many environmental factors, above all precipitation and temperature, there is a need to investigate those factors in detail. In general, climate classification depends of the average and the typical ranges of several variables, most commonly temperature and precipitation. The climate in Austria can be classified in three main climates, warm temperate climate, snow climate and polar climate (Kottek et al. 2006). In fact, the north, east and one small part of west Austria is within a warm temperate climatic zone where the weather conditions with cool summers and cold winters cause fully humid atmospheric states. Moreover, the landscapes contain hills and plains in these parts, with temperatures ranging between $-3 < T_{min} < +18$. On the other hand, the western part is well known for major and minor mountain ranges influenced by polar tundra climate, yielding colder winter weather and average annual temperature of $+10^oC$.

In the centre of Austria, from mountain range on the west to the east including Vienna, the influence of snow climate is noticeable, bringing cold winters and warm summers with ample precipitation over the year (Figure 3.1). More specifically, the mean annual temperature in the plains and hills is 15^oC, while in Alps region it is 7^oC. As expected, altitude has the biggest influence on the precipitation pattern. While in high altitude areas in the Alps region, average rainfall raises up to 2000 mm yearly, the regions in the flatlands of Austria may have only 600 mm annually (Figure 3.2).
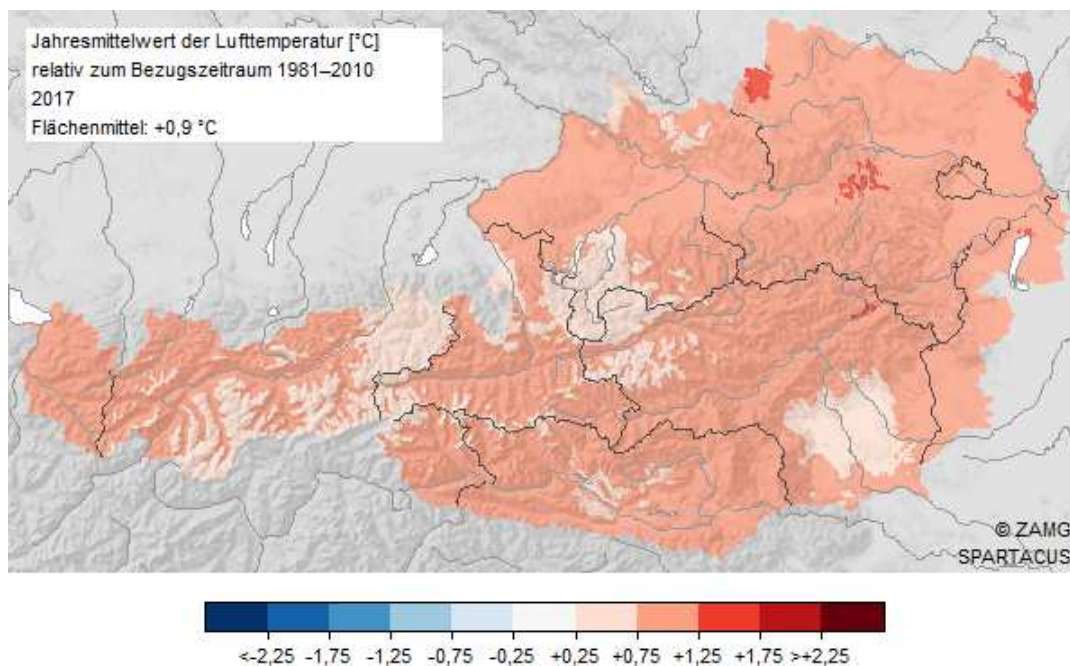
Figure 3.1: Temperature deviation for 2017 in Austria

3.1.2 Elevation

The elevation in Austria is highly variable ranging from 114 m in the east to the high mountain Großglockner with 3797 m above sea level. Due to the large difference in elevation this area can be roughly splitted into three geographical regions. The western part of Austria is mainly covered by relatively young mountains of the Alps (over 62%), the eastern part belongs to the Pannonian plain where lowlands prevail and the country's agriculture center is located. North of the Danube River is the granite mountain range, where the Bohemian Forest is situated. Even though the Alps range comes from Switzerland, the country's highest peaks are located in the central Tauern Range, which mainly slopes into the Danube River Valley as well as into the eastern lowlands. The river Danube is the most important river in Austria and the second longest river in Europe.

The Figure 3.3 represents the elevation map of Austria, showing the spatial variation in elevation between Alpine region and lowlands, as well es valleys across the country. The elevation has the significant impact on climate and temperature. For instance, in contrast to the permanent winter snow cover in the mountains above 2,500 m, in the valley below 1800 m it remains from late December through March. This causes the long wet winters in the most parts of the country.

3.1.3 Landcover

The CCI land cover map (3.4) shows the heterogeneus land cover types in Austria, represented in different colours. The lowlands in eastern part of the country, more specifically Lower Austria, Higher Austria and Burgenland are mainly covered by croplands and in some parts by broad-leaved forests. The land cover of the Alps region in the west consists mainly of needle-leaved forests with permanent ice and snow cover over about 2400 m elevation. Urban areas are mostly built next to the biggest rivers. Almost half of the country is covered with forests. Needle-leaved
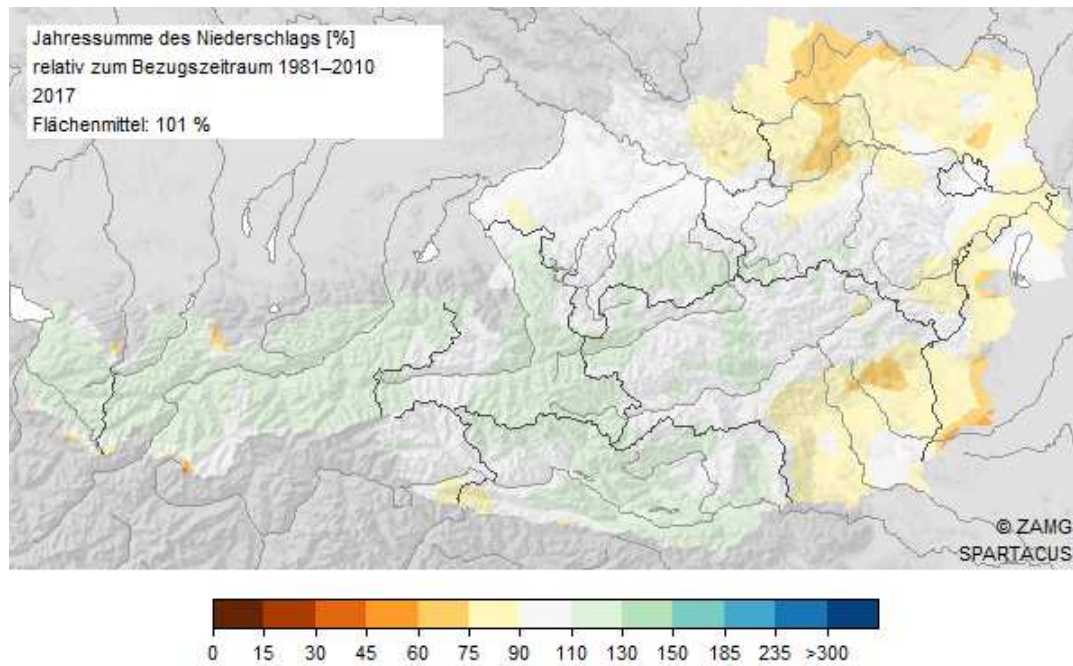
Figure 3.2: Percent of average precipitation amount for 2017 in Austria
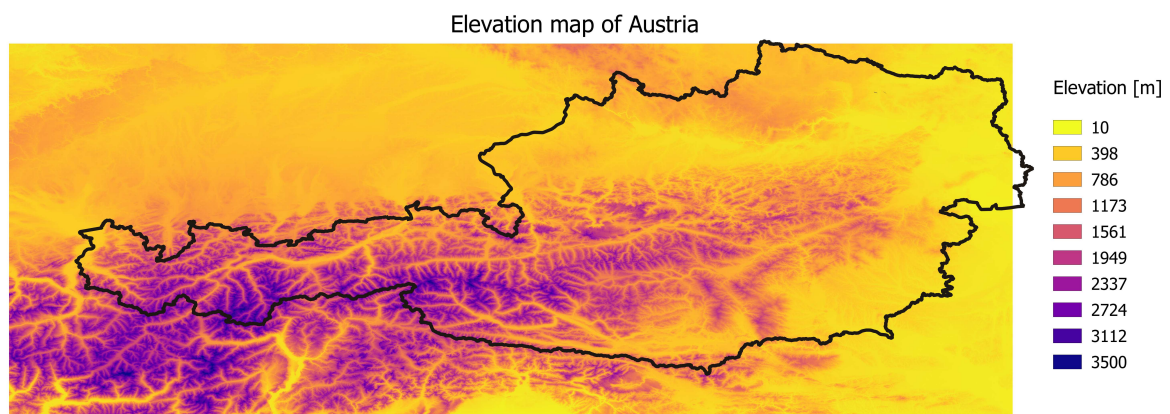
Figure 3.3: Elevation map of Austria

deciduous forests are spread in the river slopes and grassland in river valleys while broad-leaved deciduous forests can be found in a transition zone between lower mountains and hills.

3.2 Hydrological Open Air Laboratory (HOAL)

One part of the in situ data stem from the International Soil Moisture Network (ISMN) (Dorigo et al. 2011). The experimental and monitoring set-up was operated since 2013 by Hydrological Open Air Laboratory (HOAL) in Petzenkirchen. The HOAL catchment consists of 31 high quality SM sensors (4.2) installed in different soil types (Figure 4.2). Twenty of total 31 stations are permanent stations installed in grassland, forest and field edges, and 11 stations are installed in the middle of fields which are temporarily removed during harvest and other field work. From the

CCI Land Cover map of Austria

CCI LC Maps Legend

Cropland rainfed
Cropland rainfed - Herbaceous cover
Cropland rainfed - Tree or shrub cover
Cropland irrigated or post-flooding
Mosaic cropland (>50%) / natural vegetation (tree/shrub/herbaceous cover) (<50%)
Mosaic natural vegetation (tree/shrub/herbaceous cover) (>50%) / cropland (<50%)
Tree cover broadleaved evergreen closed to open (>15%)
Tree cover broadleaved deciduous closed to open (>15%)
Tree cover broadleaved deciduous closed (>40%)
Tree cover broadleaved deciduous open (15-40%)
Tree cover needleleaved evergreen closed to open (>15%)
Tree cover needleleaved evergreen closed (>40%)

Tree cover needleleaved evergreen open (15-40%)
Tree cover needleleaved deciduous closed to open (>15%)
Tree cover needleleaved deciduous closed (>40%)
Tree cover needleleaved deciduous open (15-40%)
Tree cover mixed leaf type (broadleaved and needleleaved)
Mosaic tree and shrub (>50%) / herbaceous cover (<50%)
Mosaic herbaceous cover (>50%) / tree and shrub (<50%)
Shrubland
Shrubland evergreen
Shrubland deciduous
Grassland
Lichens and mosses
Sparse vegetation (tree/shrub/herbaceous cover) (<15%)

Sparse tree (<15%)
Sparse shrub (<15%)
Sparse herbaceous cover (<15%)
Tree cover flooded fresh or brakish water
Tree cover flooded saline water
Shrub or herb. cover fl. fresh/saline/brakish w.
Urban areas
Bare areas
Consolidated bare areas
Unconsolidated bare areas
Water bodies
Permanent snow and ice

Figure 3.4: CCI Land cover map of Austria

total area of HOAL covering 66 ha, eighty-seven percent is arable land; the remaining parts are forests (6%), pasture (5%) and paved areas (2%) (Blöschl et al. 2016). This catchment is characterized by a diversity of runoff generation mechanisms. Therefore the collected data is used for examination of different runoff-, generating processes, including evapotranspiration, sediment transport, contaminant pathways, nutrient dynamics and spatial patterns in SM (ibid.).

The climate is characterised as humid with higher precipitation in summer that in winter. Mean annual temperature of 9.5^oC has been observed from 1900 to 2014 as well as a mean annual precipitation of $823 mmyr^{-1}$. The crops can be split according to the growing seasons, i.e winter and summer crops. Winter wheat and maize are mainly planted in autumn and harvested in July, where the summer crops are planted in April and harvested at the beginning of autumn. For the rest of the year, when there is no crop planted, green fertilizers are covering the fields. The seeding and harvest may vary by a few weeks from year to year, depending on the weather conditions.

3.3 WegenerNet

In addition to the HOAL SM data, in situ SM measurements collected by WegenerNet SM network (4.1) were used. The WegenerNet SM network consists of 151 stations situated around Feldbach in Styria. Twelve of 151 stations are equipped with soil sensors, measuring the SM values every hour. The sensors are installed in grassland sites and on the agricultural fields. This monitoring set-up is providing SM data since 2007.

The Feldbach lies on 281 m above sea level. The climate is warm and temperate with high precipitation during the year, even in summer months. The average annual temperature is 9.1^oC with the annual precipitation of 849 mm. The lowest average temperature of the year is measured in January with -2.1^oC while the warmest month is July with an average temperature of 19.3^oC.

3.4   BMNT

The third SM network is operated by the Bundesministerium für Nachhaltigkeit und Tourismus (BMNT) with 21 stations in total. The BMNT stations are distributed over several states in Austria, Burgenland (2 stations), Upper Austria (1 station), Styria (10 stations), Salzburg (1 station), Tyrol (5 stations) and Vorarlberg (2 stations). In this work the measurements from 21 station at the 10 cm depth were used for the comparison with RZSM layer of S1ASCAT dataset, three model datasets from hydrology, agronomy and meteorology and ensemble product.

As the stations are spread across the country, the measurements are affected by different climate and weather conditions. The stations are installed in different land cover types, mainly in the fields (16 stations), in forest (3 stations) and in meadow (2 stations). The elevation of the location of the sites ranges from 124 m in Burgenland, over 700 m in Styria and up to 1972 m in Tyrol.

Chapter 4

Data sets

4.1   EO and model data

Several datasets were used to validate SM estimates, which were compared to in situ measurements. The EO data is combined product of Sentinel-1 and Metop ASCAT product (S1ASCAT), while the three model datasets are from hydrology, meteorology and argometeorology. The ensemble was used for the comparison of groundwater observation and for validation of in situ measurements.

4.1.1   HYDRO

The hydrological soil moisture model (HYDRO) is acquired as the output of a semi-distributed hydrological model. Air temperature and precipitation from INCA are the model inputs. Integrated Nowcasting through Comprehensive Analysis (INCA) represents the high-resolution analysis and nowcasting system with a horizontal resolution of 1 km and a vertical resolution of 100-200 m. The calibration of the hydrological model is calculated by using a multi-objective calibration with in situ discharge measurements and EO SM observations. The HYDRO model yields SM values per catchment and elevation zone with a temporal resolution twice per day. The HYDRO data availability is from January 2016 - December 2018. The downscaling is carried out of 500 m sampling (Table 4.1). In comparison to other models, which provide datasets at two depths, only SM from 0-40 cm are available.

4.1.2   METEO

The meteorological soil moisture model (METEO), SURFEX, provides SM as output at two different depths, for surface soil moisture (SSM) from 0-1 cm and root zone soil moisture (RZSM) from 1-40 cm. The data is resampled at 500 m spatial resolution (Table 4.1), covering the whole of Austria. The input data of the METEO model are air temperature, wind speed and precipitation from INCA in addition to radiation components and surface pressure. The satellite data will be incorporated in the meteorological model using an Extended Kalman Filter. The time period of METEO data availability ranges from January 2016 - December 2018.

4.1.3 AGRO

The agrometeorological soil moisture model (AGRO), ARIS, provides SM at depths 0-1 cm (SSM) and 1-40 cm (RZSM). The temporal resolution of AGRO model is once daily with a 500 m spatial sampling (Table 4.1) over agricultural areas in Austria. The AGRO data is available in the period between January 2016 - December 2018. Air temperature, wind speed and precipitation from INCA, in addition to radiation are the model input and the output is one SM estimate product obtained by averaging different AGRO products. The AGRO model is processed at different land cover types; grass, maize, summer barley, sugarbeat and winter wheat, and it provides SM per land cover type.

4.1.4 S1ASCAT

The S1ASCAT Earth Observation dataset is based on radar and scatterometer data. It is a combination of Sentinel-1 backscatter and Metop ASCAT backscatter and SM estimates where the directional resampling method is applied. The underlying concept is based on temporal stability of SM: In the temporal domain SM measured at specific locations is correlated to the mean SM content of neighbouring areas, where neighbours with similar physical properties (like soil texture, land cover and terrain) show a higher coherence to the local SM than others (Wolfgang Wagner, Pathe, et al. 2008). The correlation coefficients for each local pixel are obtained by relating high resolution S1 backscatter data from a local pixel (500 m) to surrounded aggregated (12.5 km) pixels. These correlation coefficients are then used to downscale coarse-scale ASCAT SM by calculating a directional-weighted average for each local pixel. This approach is completely data driven, and therefore, no auxiliary data is needed. SM measurement unit is calculated in degree of saturation ranging from 0% (completely dry) to 100% (fully saturated). The product gives the SM estimates at two depths, SSM (0-1 cm) and RZSM (1-40 cm). The spatial sampling is 500 m (Table 4.1) over Austria with a temporal resolution of once daily. The S1ASCAT data has the longest time range of data availabily between January 2007 - December 2018, in comparison to other SM datasets.

4.1.5 Ensemble

The main product of the SM datasets is the ensemble product, which combines three model datasets and one EO SM product (sec. 4.1.4). The three SM model products are model outputs from a hydrological (sec. 4.1.1), meteorological (sec. 4.1.2) and agrometeorological (sec. 4.1.3) model. The ensemble product is calculated using a poor man's ensemble for two years (January 2016 - December 2018), providing the SM estimates at two depths, SSM and RZSM. The poor man's ensemble is a method, which is often applied to independent numerical weather prediction model forecasts (Ebert 2001). This method performs multiple model integrations, where intensive computing resources are not required. The spatial resolution of ensemble is available on 500 m and 100 m (Table 4.1). The 100 m sampling product is downscaled using a hydrological downscaling method.

Resolution	Ensemble	HYDRO	METEO	AGRO	S1ASCAT
temporal [daily]	once	twice	twice	once	once
spatial [m]	100 m / 500 m	500 m	500 m	500 m	500 m

Table 4.1: Temporal and spatial resolution of datasets

4.2 Ground data

4.2.1 In situ soil moisture data

The validation of the SM datasets has been carried out over several test regions in Austria (Fig. 4.1). A SM monitoring networks were set up to provide information about the effect of small-scale variability of topography variations and to help us to understand this effect on microwave response of satellite sensors.

Figure 4.1: Spatial distribution of SM networks - BMNT, WegenerNet and HOAL

4.2.1.1 HOAL

One of the test regions is the experimental agricultural catchment in Petzenkirchen, Lower Austria, which is equipped with a SM network (HOAL SoilNet) since 2013 (Fig. 4.1). The Hoal SM network consists in total of 31 stations, where 20 permanent stations are installed in pasture and forest and 11 temporary stations in the agricultural fields (4.2). The SM variations are captured using time domain transmission sensors installed at four depth below ground surface. Measurements are taken at 5, 10, 20 and 50 cm depending on particular in situ SM station at the temporal resolution of 30 min with additional temperature measurements at mentioned four depths (Blöschl et al. 2016). The SSM products are validated using the sensor data at 5 cm depth. For the validation of RZSM, the data at 20 cm depth was used as a reference. The reason for this is, that most of in situ SM stations have sensors at 20 cm depth and in order to be able to make a relevant comparison with other products all further analysis has been calculated with this values.
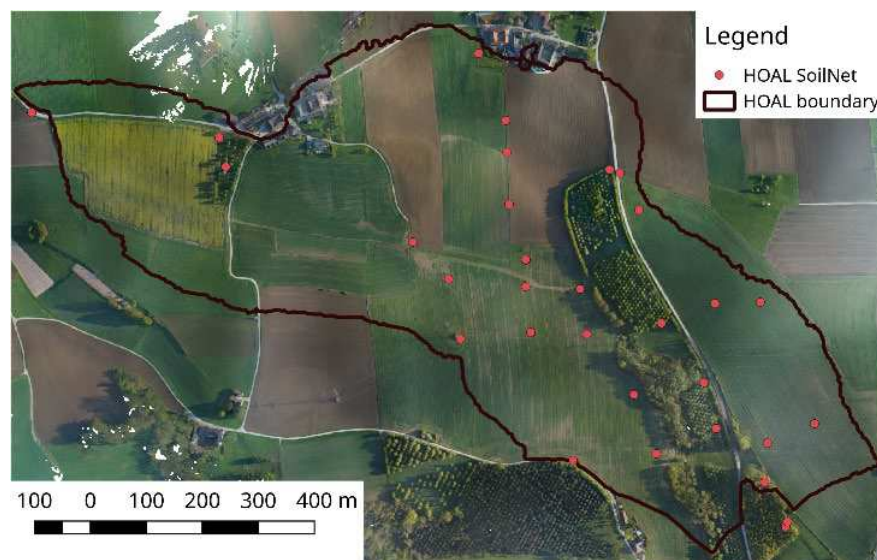
Figure 4.2: Map of the HOAL catchment and SoilNet stations

4.2.1.2 WegenerNet

In addition to the SoilNet, in the analysis were used measurements from the WegenerNet SM network. The WegenerNet network contains 151 stations in total, where twelve of them are equipped with soil sensors. The soil sensors are measuring pF-value and temperature using pF-Meter. The pF-Meter's measurement parameter is the pF-value, which is characterized as logarithm of the absolute value of soil metric potential (J. Fuchsberger n.d.). The WegenerNet SM stations are measuring SM since 2007. The time span for SM data provided for this research ranges between October 2013 until December 2019. SM is measured on an hourly basis at the 20 cm depth beneath the surface of the ground. The overview of the spatial distribution of WegenerNet, BMNT and HOAL SM stations is presented at the spatial map (Figure 4.1).

4.2.1.3 BMNT

The in situ SM data collected by BMNT SM network, besides WegenerNet and HOAL SM network, served as a reference data for the validation of the model products, S1ASCAT product as well as of the ensemble. In total 21 BMNT SM stations are installed in different regions across Austria measuring the SM estimates over several land cover types. Several stations are measuring SM variation with weighing lysimeter and one station contain norm lysimeter. Weighing lysimeter reveals the amount of water crops use by repeatedly weighing a great block of soil in a field in order to detect and capture reduction of SM. For the other station no information about the type of the station was available. Depending on the specific station, the measurements of SM variations are estimated every hour and in most cases on 6 different depths (10, 15, 20, 25, 30, 40, 45, 50, 60, 70, 80, 90, 100, 110, 120, 140, 145, 150, 180, 200 and 300 cm). All BMNT SM stations have sensors at 10 cm depth and therefore these measurements were used in the validation analysis These measurements were compared with RZSM layer of S1ASCAT, three model datasets and ensemble. As the stations are spread in many regions and soil types, the overall

result of the analysis is more representative. In this work the SM data was provided from January 2015 until Mai 2019.

4.2.2 Groundwater

In addition to standard comparison and validation of SM, in this work the novel approach is implemented containing the extended validation of the ensemble product with a groundwater dataset. The groundwater data provides a critical additional dimension to this work. The data is provided from the BMNT, which has maintained a functioning network of groundwater stations over more than thirty years. The groundwater stations are located irregularly over whole Austria. Each groundwater station in equipped with a remote data transmission and the data are sent once daily to the BMNT (Land and Forestry Data Center - LFRZ). In the next step the daily mean from the data of the remote groundwater measuring points are calculated. The data provided for this analysis is stored on daily basis, representing the groundwater layer depth above sea level. The groundwater data is available for over 4000 sites in Austria, which are located in most cases next to the rivers or lakes. The map (4.3) presents an overview of the spatial distribution of groundwater stations in Austria. The groundwater data with significant deviation was filtered and excluded from further analysis as described in section 5.1.1. The groundwater level values of 2670 stations were used for comparison with SM values from the ensemble product. The time span of groundwater data availability ranges between January 2016 and December 2019.
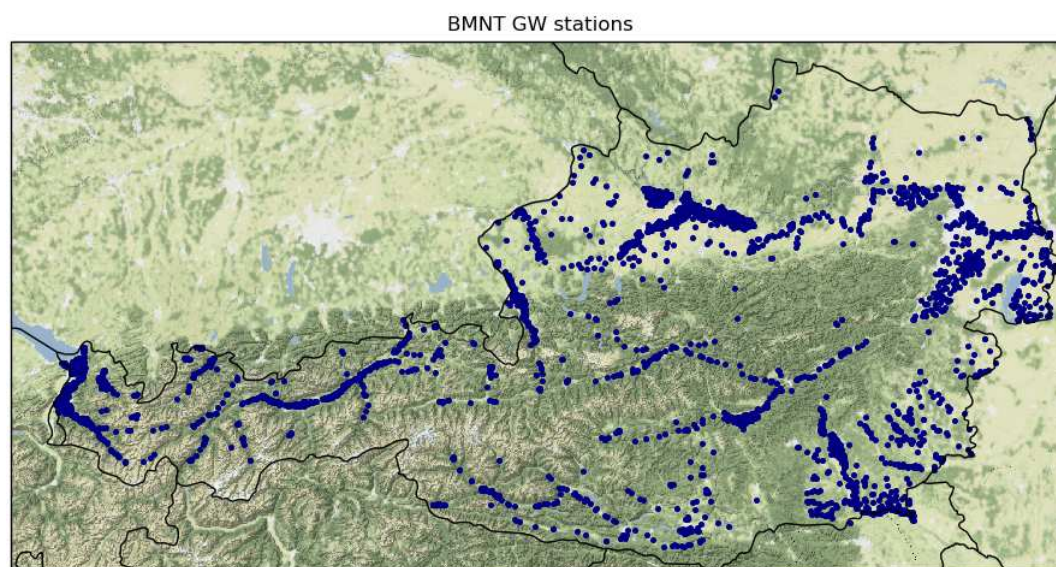

Figure 4.3: Spatial distribution of groundwater stations in Austria

4.3 Auxiliary data

Auxiliary data is used to mask the EO and model data. In order to complete the final explanation of the results of the validation and the evaluation, the data of land cover and porosity was used.

4.3.1 Era5

Era represents the climate reanalysis produced by European Centre for Medium-Range Weather Forecasts (ECMWF). The last of five projects of Era is Era5, which dataset is covering the period 1950 to present. The main aim of climate reanalysis is to generate consistent time series of multiple climate variables. This is done by combining past observations with models. The Era5 provides hourly estimates of many atmospheric, land and sea climate variables together with estimates of uncertainty from 1979 to present. The data is available on regular latitude-longitude grids at 0.25^o x 0.25^o resolution (30 km grid), with atmospheric parameters of 137 pressure levels from the surface up to a height of 80 km (Hersbach et al. 2019). Era5 variables are produced at the surface and on the model levels. In this work the Era5 temperature, snow cover height and precipitation data is used for masking the datasets.

4.3.2 CCI LC Map

The Climate Change Initiative (Hollmann et al. 2013) has been established by the European Space Agency (ESA) in order to create climate data records for essential climate variables (ECVs). These records are freely accessible representing different ECV projects, i.e. sea level, sea surface temperature, land cover, glaciers, soil moisture and others. The aim of CCI is to use the full potential of the long-term Earth Observation (EO) archives and to provide products for climate modelers. One of the main reasons for this initiative is the increasing use of satellite data to calibrate different models on space and time scales. The heterogeneous land cover map is visible in Figure 3.4 with the legend which enables to easily distinguish between different land cover types. The spatial resolution of the CCI land cover map is 300 m and the plotted data is from 2010.

4.3.3 Porosity

In order to be able to extend the analysis of the microtopography effects (Dunne, Zhang, and Aubry 1991) on the SM variations, geophysical parameters of the surface have been investigated in a more detailed way. Various interlinked underlying driving processes cause the changes in geophysical parameters which implies changes in surface properties. As it is already mentioned in Introduction, the main driving processes for SM variations are meteorological nature, as evaporation and precipitation. However, it is important to take into account the impact of surface nature to the differences in SM. Surface properties can be divided in soil texture and land cover type. Soil texture is regulated by the relative proportion of sand, silt and clay sizes that form the mineral fraction of the soil. Due to the influence of soil texture to the supply of water in the soil and the water movement in the soil, it is responsible for velocity of infiltration rates. The land cover type influences differences in water uptake and from the topographic perspective, the hill slopes cause different vertical moisture redistribution. The CCI land cover map (3.4) indicates the diversity of land cover types in Austria, specially in the central part, where occurs the transition between Eastern Alps and lowlands from west. In this region the highest porosity values can be found (4.4). The higher porosity values are distributed along the biggest river valleys and northeast of the Danube River. The data for

the porosity values is provided from International Soil Reference and Information Centre (ISRIC) in 250 m spatial resolution.
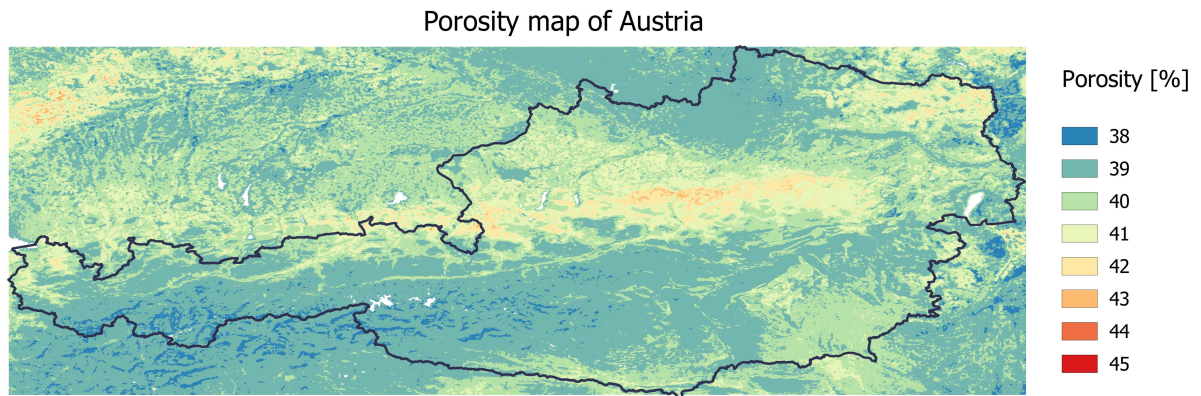

Figure 4.4: Porosity map of Austria

Chapter 5

Methods

The investigation in this research involved sampling and analysing six types of SM datasets to capture changes in SM over Austria. The in situ measuring stations are located in different regions (see Figure 4.1) covering several types of land cover. The in situ data was used as a reference for the validation of the three model datasets, the S1ASCAT product and the ensemble. The groundwater data was used to evaluate the ensemble product. As already mentioned in section 4.1, in this work the analysis between in situ observations and model, S1ASCAT and ensemble datasets was computed using the SM data collected at two layer depths, SSM as a top ground layer and RZSM with a layer depth at 20 cm. For the validation of ensemble with groundwater dataset, the RZSM layer of ensemble SM dataset was compared to changes in groundwater level.

5.1 Pre-processing

It is well known that some natural effects, such as snow cover, temperature and frozen soils can potentially hamper the EO and in situ SM measurements. Therefore, various pre-processing steps are required before the validation metrics can be computed. The following section briefly summarizes the steps that were applied to the datasets before the validation analysis was carried out.

5.1.1 Filtering the groundwater data

Over 4000 of groundwater datasets were available for the comparison with the ensemble dataset. As some of groundwater data showed significant deviation, they were filtered and excluded from further analysis. The deviation was identified by comparing the difference between arithmetic means of two years with the standard deviation of one year. After filtering, the datasets of around 2600 stations were implemented in this analysis. This additional groundwater dataset is much larger than any of in situ SM network used in this work, and therefore it provides a broader comparison with high resolution SM estimates.

5.1.2 Masking

In order to include only reliable SM measurements in the validation, values collected under frozen conditions were masked out in all datasets. Air temperature and snow

cover values obtained from the ERA5 dataset (4.3.1) are used as reference data. All days with negative mean temperature are excluded from further analysis. The masked data is expected to occur in winter months which can be seen in the Figure 5.1. The masking is applied after temporal matching. The Figure shows the non-masked and the masked time series of two different SM datasets.

(a) Masking not applied   (b) Masking applied
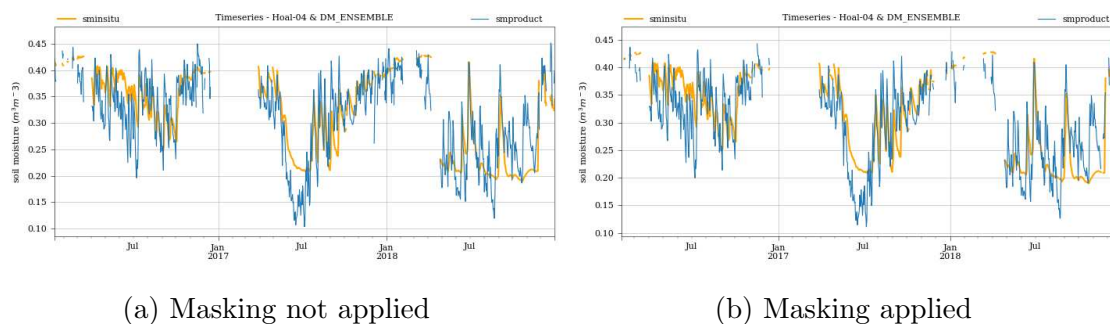
Figure 5.1: Temporally matched two datasets and masked out for frozen conditions

5.1.3 Temporal matching

5.1.3.1 In situ soil moisture

As the temporal resolution and time stamps of the different products (S1ASCAT, three model datsests and ensemble dataset) and in situ datasets differ, all datasets are temporally resampled before the validation can be carried out. More specifically, for the datasets that are provided with twice daily time stamp (see Table 4.1) the arithmetic mean was calculated in order to obtain one single value per day. Lastly, the temporal matching was computed by matching measurements from every single in situ station with each product dataset (S1ASCAT, three model datasets and ensemble dataset) within a window of 24 hours. All validation results presented in this work were calculated from average daily SM. The spatial matching between in situ stations and INCA grid from the S1ASCAT, model data and ensemble dataset was performed by a nearest neighbour search where the coordinates of the in-situ measurement sites served as reference. The INCA grid repesents the high resolution product of trilinearly interpolated forecast of numerical weather prediction model (Steinheimer and Haiden 2007). Moreover, the temperature, snow cover and precipitation datasets were temporarily matched with every comparison of in situ measurements with each product dataset (S1ASCAT, ensemble and three model datasets).

5.1.3.2 Groundwater

For the groundwater data, the temporal matching was performed by matching observations from each groundwater station with ensemble dataset within one day. Additionally, the temporal matching with temperature, snow cover and precipitation data was computed for every single comparison with groundwater observations.

5.1.4 Scaling

The in situ data is originally expressed in volumetric SM ($\mathrm{m}^3/\mathrm{m}^3$). The ensemble and METEO model SM datasets are characterized by the same measurement units as in situ data. However, the S1ASCAT, HYDRO and AGRO product datasets range between 0 and 1 and they are expressed by relative SM (degree of saturation(%)). A conversion between the different units is possible by multiplying the degree of saturation with the respective porosity value of the location. However, as no sufficiently accurate soil information is available, S1ASCAT, ensemble and three model datasets have been scaled to the reference in situ data using a mean standard deviation scaling method 2.2.1. The scaling method was not applied for the ensemble product when comparing to groundwater data as the soil moisture content in measured in $\mathrm{m}^3/\mathrm{m}^3$ and groundwater in meters above sea level.

5.1.5 Anomaly calculation

In order to avoid seasonal effects, anomaly time series based on the climatology are calculated. The climatology show the seasonality, which is the presence of variations that occur at specific regular interval, i.e. yearly, monthly. It also represent the long-term average, the mean of several years. In order to obtain anomaly values the difference between raw time series data and climatology values was estimated.

5.2 Validation with in situ soil moisture

Error characterization and validation play an essential role in estimating the accuracy and reliability of a given dataset. In order to be able to properly quantify the SM products (S1ASCAT, ensemble and three model datasets) on their reliability, several statistical validation scores were calculated. In this analysis the main aim was to validate the accuracy of the high resolution SM parameter estimates. This is done by comparing S1ASCAT, ensemble and three model datasets with in situ SM measurements, where the in situ measurements were used as reference. The comparison is done by calculating standard validation metrics which characterize if there exists any agreement or disagreement between two compared datasets.

5.2.1 Temporal analysis

In this analysis, two standard validation metrics were computed for the purpose of direct comparison between the in situ SM measurements and ensemble, S1ASCAT and three model datasets. They represent standard metrics to access the accuracy of remote sensing measurements with respect to true fields. As the linear statistical dependency between these two datasets is expected, the Pearson correlation coefficient (2.3.1.1) was calculated. Second validation metric is uRMSD (2.3.2.1) and its value is mainly driven by random errors of the dataset. The uRMSD represents the bias as the difference of the long-term mean between measured and predicted SM and it is found to be the target metric of evaluation the SM product of diverse satellite missions (Colliander et al. 2017). The temporal dynamics of the five SM datasets were validated by computing these two metrics of every comparison between measurements of each in situ SM station with S1ASCAT, ensemble and three

model datasets. This procedure has been performed for both raw time series and the anomalies (5.1.5). While the raw time series contain absolute SM values, the mean seasonal SM cycle has been subtracted from the anomaly time series. Consequently, the metrics calculated on the raw time series evaluate the overall representation of SM, while the anomaly metrics show how well the products capture rainfall events and the subsequent dry-down without the additional effect of the seasonal SM cycle.

In addition, the calculation of Pearson correlation coefficient and uRMSD was not only computed for raw time series and anomalies, but also for each season individually (winter: December, January, February; spring: March, April, May; summer: June, July, August; autumn: September, October, November) for the entire time period 2016-2018. Due to S1ASCAT data availability since 2007, and in situ measurements collected from Hoal, WegenerNet and BMNT SM network since 2013, 2013 and 2015, respectively, the temporal matching between them depends of time range of in situ SM data availability. The validation procedure was carried out for every in situ station compared to S1ASCAT, ensemble and three model dataset of the spatial resolution of 500 m at two layer depths (SSM and RZSM). Only exception was the HYDRO dataset, where the data was provided for RZSM layer. This procedure was applied on both raw time series and anomalies. In addition, in order to aid the validation, the comparison between the temporally matched datasets of in situ SM mesurements and downscalled ensemble product (100 m spatial resolution) was conducted. Lastly, the mean of Pearson correlation coeffiecient and uRMSD of raw time series and anomalies (for entire period and for every season separately) of all three in situ SM networks was calculated.

5.3 Evaluation of groundwater

The final analysis is extended with an additional novel approach by comparing and evaluating groundwater observations with ensemble dataset, which provides more insights into the reliability of high resolution SM estimates.

5.3.1 Temporal analysis

The groundwater dataset and ensemble data were compared in novel manner, using different metrics. While the Pearson correlation coefficient characterises linear statistical dependency between two datasets, the Spearman's correlation (2.3.1.2) requires no normality. Based on the assumption of non-linear correlation between groundwater dataset and ensemble product, the Spearman's correlation metric was calculated. The uRMSD (2.3.2.1) values represent the matching between the residues of groundwater time series to the ensemble time series after removal of the bias, as they are representing the same phenomenon (Los 2009).

With the intention of identifying the response delay of groundwater observation, the Spearman correlation coefficient within the each lag in a range of 10 days for the period of 180 days were calculated. The lag with the highest Spearman correlation coefficient is expected to provide the delay time of groundwater response to precipitation events. The lags were calculated in period of six months (every 10 days) for every comparison between measurements of each groundwater station with ensemble dataset.

(a) Smooth signal course
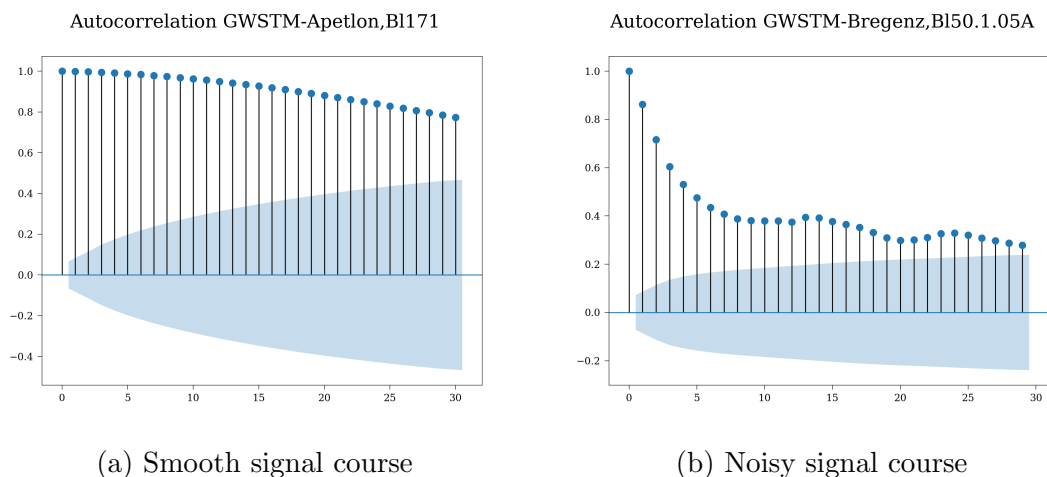
(b) Noisy signal course

Figure 5.2: Autocorrelation of two groundwater stations

To better understand the evaluation results between SM and groundwater, two metrics were calculated for the groundwater data. First one is the autocorrelation (Huitema and Laraway 2006), which described the correlation between groundwater time series at two different points in time, as a function of delay. The mean autocorrelation for the first 15 days was calculated. The aim of calculating the autocorrelation of groundwater is to detect if repeating patterns of the singe observation occurred. The results of autocorrelation provided information on the temporal behaviour of the groundwater. Either very quick changes occur in groundwater time series or it is characterized as smooth course, which implies that the response of the groundwater station is delayed much longer in comparison to SM estimates from ensemble product (Figure 5.2). The resulting output of autocorrelation can range from 1 to negative 1, where 1 represents perfect positive correlation (the same pattern is repeated in both points in time of the same timeseries) and -1 indicates the perfect negative correlation (pattern of one timeseries is disproportionate to the pattern of delayed timeseries).

In order to make the ensemble estimates more comparable to groundwater data, the rolling mean was applied to smooth out the short-term fluctuations in ensemble time series data and to highlight long-term trends. The rolling mean (or moving averages) is used for a period of 15 days.

In general, the standard deviation of differences between two points provide the insight into the sensitivity of observations to capture small variations in particular phenomenon. First the difference between two points for the whole time series was calculated and then the standard deviation of the differences. By comparing this estimate of two independent datasets it reveals if they react similar to the same phenomenon, i.e. precipitation event or evapotranspiration. In this research, the standard deviation of differences between two points is the second metrics which was quantified to investigate the temporal behaviour of the groundwater. With this metric it is expected to obtain higher value when the groundwater level data capture small variations and fast responses to the rainfall events while the other groundwater data is manifested though smooth behaviour with a lag delay. These two metrics were used together with groundwater depth to surface in order to explain correlations between SM and groundwater. Furthermore, the averaged groundwater depth (2.1.2) was used for the deeper analysis in order to detect and explain correlations

between SM variations and the effect of groundwater depth to groundwater changes. Additionally, the groundwater layer depth was calculated as the difference between surface height and median of whole raw time series.

To sum up, the four validation metrics were used to compare each groundwater station against ensemble product. There metrics are Spearman correlation coefficient, uRMSD, autocorrelation of groundwater data, and standard deviation of differences of groundwater measurements. The averaged groundwater depth provided more insights into the relationships when ensemble SM estimates were compared to groundwater dataset at higher depths and when the groundwater is close to the surface. If the groundwater is quite near to the surface then it is most likely to observe very good response on rainfall events, while for the deep groundwater the lag is expected, which represents the time delay that water needs to reach the station. In addition to the temporal analysis, a spatial analysis was formulated by relating the results to the CCI land cover map and porosity values across the country.

Chapter 6

Results

The evaluation of the ability of high resolution SM products to retrieve reliable soil moisture estimates is presented in this chapter. The validation was performed in a twofold manner: first, by comparing ensemble dataset, three model datasets and S1ASCAT dataset with in situ soil moisture measurements; and second, by comparing ensemble dataset with groundwater measurements. The results of the analyses outlined in previous chapters is briefly described in following sections.

6.1 Soil moisture validation

6.1.1 HOAL

Figure 6.1 shows one example of time series comparison between one in situ measurement station from Hoal network (Hoal-04) and four soil moisture products. The bias of AGRO product shows a trend to considerably underestimate SM during the summer period while the HYDRO product slightly overestimates in the same period. As the HYDRO data was only available for Petzenkirchen (Hoal network), there was no possibility to compare it to the results of other SM networks. There is highly probable that the bias is linked to the mean-standard scaling method (2.2.1) used to scale S1ASCAT, model and ensemble data to the in situ measurements. The seasonal cycle is visible in every comparison but varies due to many interannual variations caused by the rainfall conditions.

The METEO product shows little underestimation of in situ estimates. A considerable underestimation is visible in 2016 when comparing AGRO, METEO and S1ASCAT datasets with in situ time series. This can be explained due to more rainfall events in the summer 2016 which caused wetter summer and therefore the curve in this year raises later than in other years.

The S1ASCAT raw time series followed well the temporal dynamics and the seasonal pattern of the in situ measurements. In order to evaluate the ability of S1ASCAT and in situ datasets to capture short-term scale soil moisture variations, the anomalies were calculated and displayed in Figure 6.2. The fairly good correspondence with S1ASCAT data is visible. Due to humid climate in this region with a highest precipitation in July, the peak in rainfall events is particularly visible in summer months.

In general, a satisfying agreement between Hoal SM estimates, measured in agricultural catchment, and ensemble dataset is visible. Figure 6.3 shows the time series

Figure 6.1: Example of raw time series of permanently installed in situ Hoal-04 station RZSM and 4 products (500m). a) AGRO, b) S1ASCAT, c) HYDRO and d) METEO. In addition to SM, rainfall measurements are displayed.
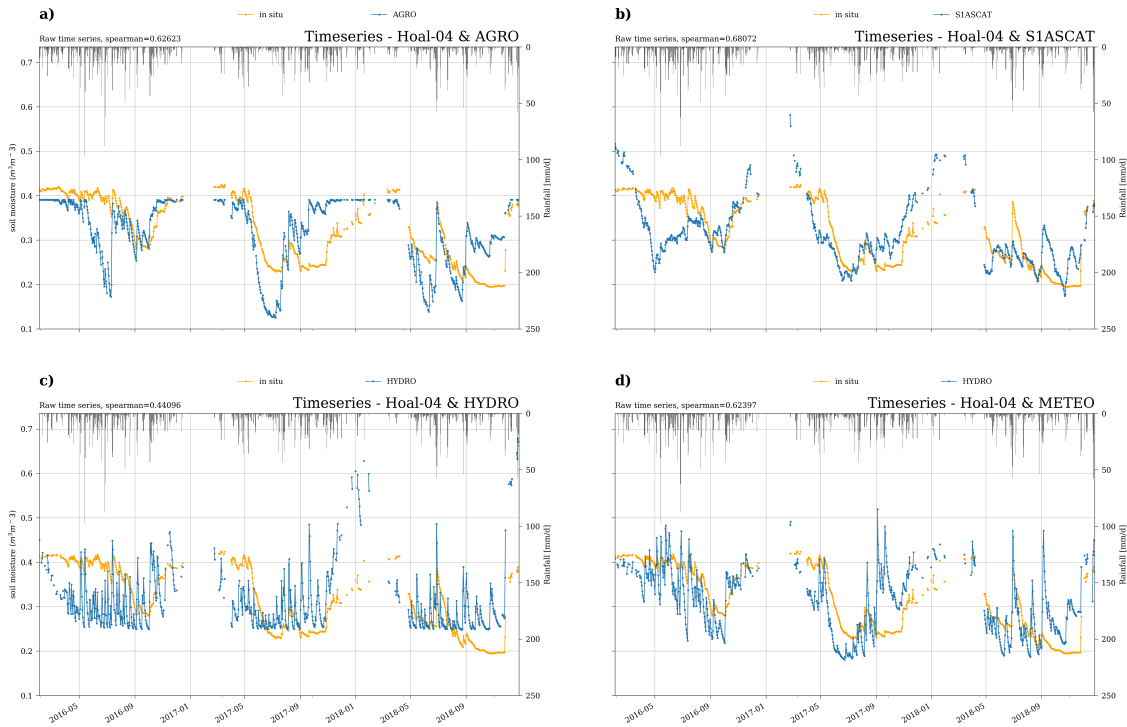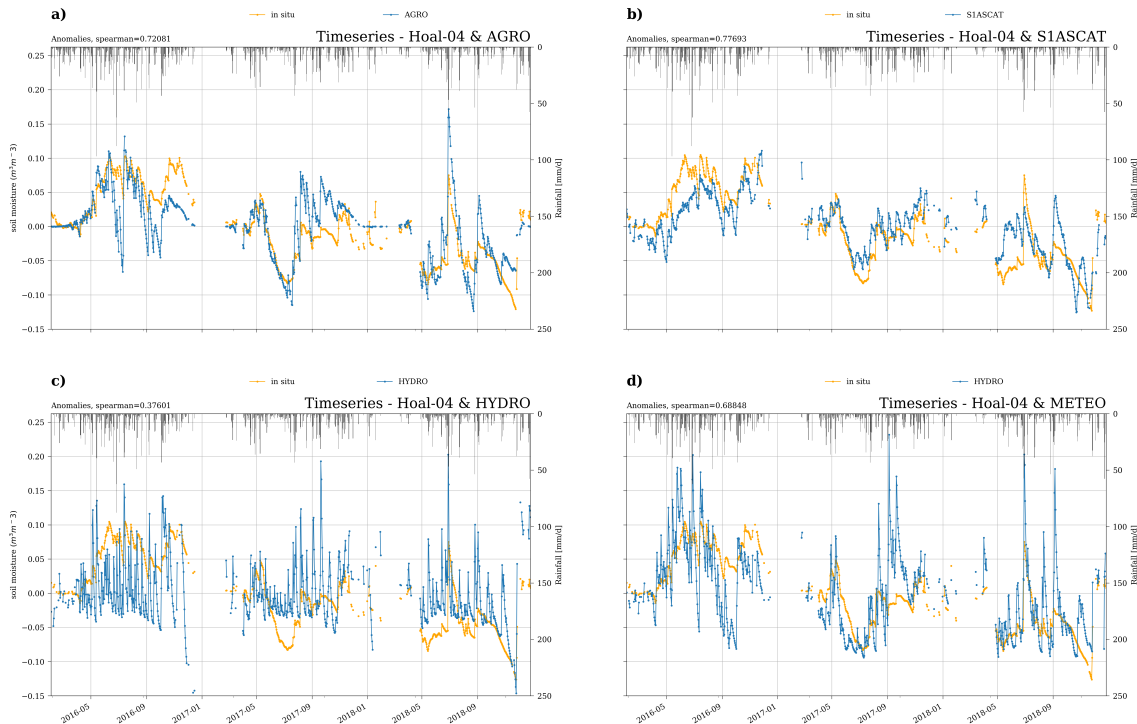

Figure 6.2: Example of anomaly time series of the permanently installed in situ Hoal-04 station RZSM and 4 products (500m). a) AGRO, b) S1ASCAT, c) HYDRO and d) METEO. In addition to SM, rainfall measurements are displayed.

and anomalies of Hoal-04 measurement station compared to ensemble with the spatial resolution of 500 m. The ensemble product responds fairly good to precipitation events, even though it was not able to fully cover SM dynamics and drying phases in summer months. This can be explained due to inability of satellite observations to penetrate through dense grass vegetation because this station is permanently installed in orchard, where the height of the grass in the late summer-autumn was most likely very high. The differences between raw time series and seasonality can be found on the anomaly plot, where the anomalies of ensemble product indicate very noisy course of time series. It can be assumed that one part of this noisy behaviour come from sensitivity of remotely sensed data to atmospheric and sensor effects, as well as to the vegetation density. Moreover, HYDRO dataset shows the similar behaviour. The appreciable R_p value of 0.65 for raw time series and even higher for anomalies indicates an improved agreement for the ensemble product with in situ data.
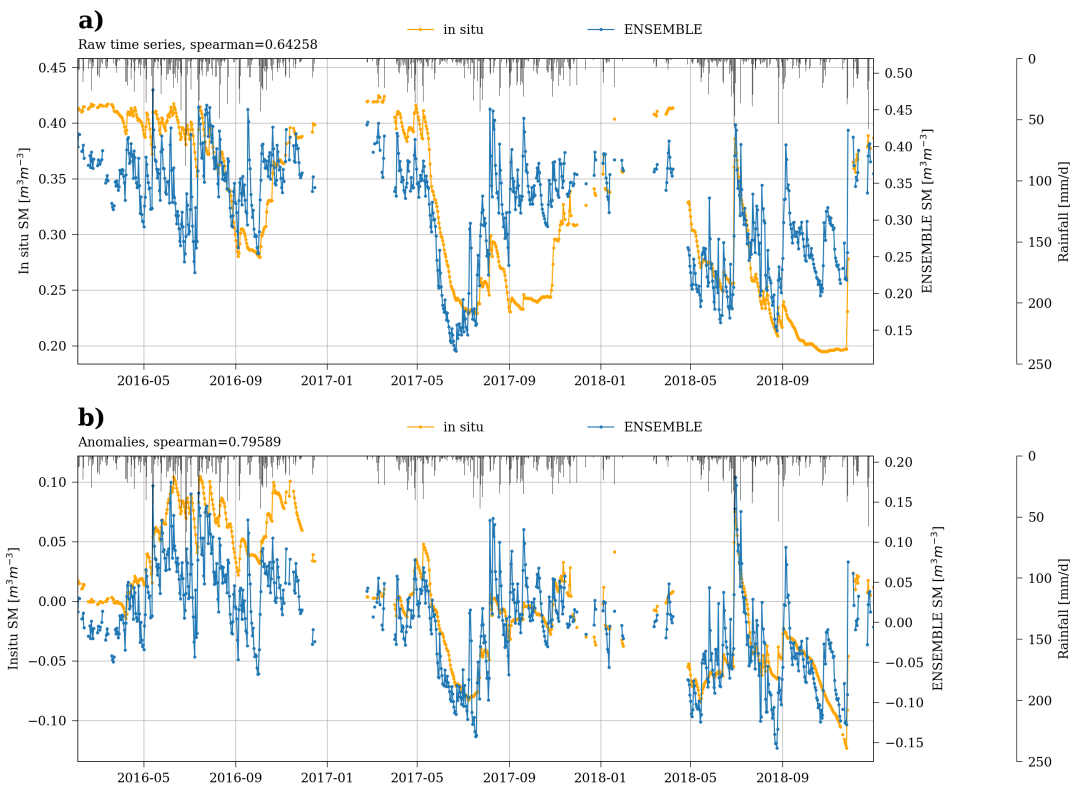

Figure 6.3: Example of a) raw and b) anomaly time series of ENSEMBLE and permanently installed in situ Hoal-04 station RZSM (500m). In addition to SM, rainfall measurements are displayed.

Due to the fact that even if the in situ data represents the reference data for this analysis, it is point scale measurement and not necessarily representative for the whole satellite footprint observation. Therefore, it is necessary to compare these results to another in situ station, which was temporary installed in a different crop type, in the agricultural field. While the first station (Hoal-04) was permanently installed in orchard, the Hoal-25 measured SM values every year in different crop types. These differences of crop types in every year are evident in Figure 6.4, where the rapeseed was planted in 2016, and maize and wheat in 2017 and 2018, respec-

tively. As the precipitation rate was very high in 2016, the ensemble dataset shows a trend to underestimate in situ records from Hoal-25 station in spring and summer months more than in other years. In summers 2017 and 2018 significant matching response to SM variations can be identified of ensemble dataset and measurements from temporary installed in situ station. Moreover, almost every rainfall event was captured from both products.
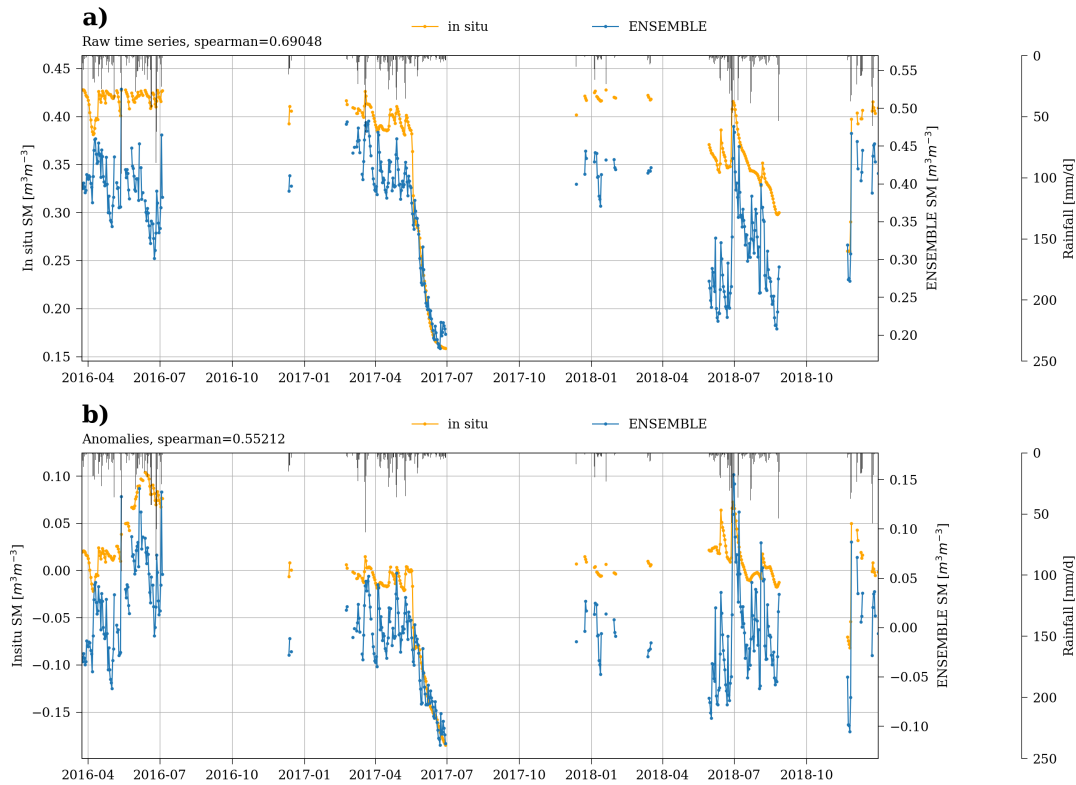

Figure 6.4: Example of a) raw and b) anomaly time series of ENSEMBLE and temporary installed in situ Hoal-25 station RZSM (500m). In addition to SM, rainfall measurements are displayed.

Over the entire time period, for the Hoal network the correlations range between 0.39 and 0.71 for the individuals products (raw time series). Table 6.1 shows the correlation values of SSM layer, while the correlations of RZSM are summarised in Table 6.2. The correlations between SSM and RZSM layer for the Hoal network do not show any big difference. The highest Pearson correlation coefficient of 0.92 is calculated by comparing agrometeorological model dataset with estimates measured by temporary installed station Hoal-11 at the RZSM layer and 0.81 for SSM. This station has very high correlations compared with ensemble dataset (0.81 for SSM and 0.84 for RZSM), meteorological model dataset (0.58 for SSM and 0.71 for RZSM), hydrological model dataset (0.44 for RZSM) and slightly lower correlation with SSM of S1ASCAT dataset (0.15 for SSM and 0.6 for RZSM). The in situ Hoal-17, permanently installed station in forest, show lowest correlations when comparing to hydrological model dataset (0.2 for RZSM) and slightly better agreement with datasets of meteorological model (0.43 for SSM and 0.51 for RZSM), agrometeorological model (0.47 for SSM and 0.52 for RZSM), ensemble (0.51 for SSM and 0.41 for RZSM) and S1ASCAT (0.45 for SSM and 0.58 for RZSM). The significant

differences in correlations are visible when comparing with S1ASCAT SSM dataset and with HYDRO RZSM dataset. The reason for these differences in S1ASCAT dataset is most likely due to different sensitivity levels of in situ sensors and microwave sensing to the soil's surface. As the HYDRO model is calculated using calibration with several input data, among other things, with EO SM estimates, it is very probable that EO data showed discrepancies due to inability to penetrate through sparse forest.

Time	Type	Ensemble		METEO		HYDRO		AGRO		S1ASCAT	
		Rp	uRMSD	Rp	uRMSD	Rp	uRMSD	Rp	uRMSD	Rp	uRMSD
Full time	Abs.	0,708	0,048	0,618	0,054			0,689	0,049	0,558	0,058
series	Ano.	0,569	0,028	0,469	0,039			0,613	0,020	0,406	0,035
Winter	Abs.	0,152	0,032	0,113	0,031			0,188	0,023	0,296	0,041
(DJF)	Ano.	0,495	0,020	0,501	0,019	No SSM data available from HYDRO		0,504	0,011	0,533	0,028
Spring	Abs.	0,685	0,038	0,632	0,041			0,685	0,036	0,446	0,054
(MAM)	Ano.	0,501	0,026	0,514	0,029			0,529	0,020	0,404	0,035
Summer	Abs.	0,713	0,038	0,520	0,057			0,728	0,035	0,403	0,045
(JJA)	Ano.	0,617	0,030	0,478	0,053			0,706	0,021	0,289	0,033
Autumn	Abs.	0,785	0,036	0,600	0,046			0,840	0,031	0,575	0,051
(SON)	Ano.	0,688	0,028	0,598	0,035			0,824	0,018	0,464	0,038

Table 6.1: Validation metrics of 500m products compared to Hoal SM network (SSM)

Time	Type	Ensemble		METEO		HYDRO		AGRO		S1ASCAT	
		Rp	uRMSD	Rp	uRMSD	Rp	uRMSD	Rp	uRMSD	Rp	uRMSD
Full time	Abs.	0,676	0,042	0,647	0,043	0,385	0,062	0,705	0,041	0,606	0,049
series	Ano.	0,493	0,024	0,439	0,026	0,390	0,027	0,572	0,015	0,469	0,017
Winter	Abs.	0,263	0,022	0,237	0,026	0,126	0,069	0,344	0,014	0,301	0,044
(DJF)	Ano.	0,563	0,015	0,439	0,019	0,720	0,024	0,716	0,009	0,256	0,017
Spring	Abs.	0,743	0,027	0,721	0,030	0,433	0,033	0,773	0,023	0,540	0,044
(MAM)	Ano.	0,452	0,019	0,554	0,019	0,355	0,023	0,449	0,011	0,533	0,015
Summer	Abs.	0,732	0,037	0,662	0,034	0,280	0,036	0,760	0,029	0,633	0,033
(JJA)	Ano.	0,554	0,031	0,517	0,030	0,180	0,025	0,703	0,016	0,392	0,015
Autumn	Abs.	0,669	0,041	0,622	0,040	0,652	0,042	0,748	0,025	0,586	0,041
(SON)	Ano.	0,574	0,033	0,580	0,029	0,565	0,036	0,667	0,016	0,537	0,018

Table 6.2: Validation metrics of 500m products compared to Hoal SM network (RZSM)

The analysis is improved by calculating the correlations for four seasons. It is apparent from the correlations that the seasonal metrics in autumn report very high correlations of up to 0.84 (raw time series - SSM) and 0.75 (raw time series - RZSM). Slightly lower correlation are observed in spring and summer. The reason for these differences is believed to be due to the lower precipitation rate and soil's ability to absorb water. The correlations in winter months are noticeably lower which can be explained by a small number of observation due to the masking procedure for frozen conditions and snow cover.

In addition to the correlation, the uRMSD was calculated in order to obtain additional information about the accuracy between in situ SM measurements and

S1ASCAT, ensemble and three model datasets. The target accuracy of $0.04 m^3 m^{-3}$ volumetric SM as a commonly used threshold in SM validation studies was fulfilled in every comparison in RZSM layer except for S1ASCAT where it is slightly above. For the SSM layer, the highest uRMSD estimates are of S1ASCAT product of $0.06 m^3 m^{-3}$ while the estimates of other products meet its expected performance. In general, the calculated metrics for Hoal catchment can be assumed to show very good temporal agreement with all five SM product (S1ASCAT, ensemble and three models) and therefore the retrieved estimates of the ensemble product are accepted as highly reliable.

6.1.2 WegenerNet

In addition to the Hoal SM network, the SM in situ network WegenerNet was used as a reference for the extended validation. In order to compare the quality of SM estimates of ensemble, S1ASCAT and two model data sets with in situ measurements, datasets of 4 stations, that were temporal and spatial matched with all four SM datasets, were used in this analysis. These 4 stations contain installed sensors at 20 cm depth, which are placed in the grassland and on the agricultural fields on the flat land (281 m). As the data of sensors at the depth of 20 cm is provided, the standard validation metrics were calculated for RZSM layer (6.3). Comparing the results between ensemble and other products, it is evident that the S1ASCAT product provides slightly better metrics values. The correlations are not high, which is most likely caused by the low number of stations and not very reliable in situ sensors. Very often just one station represents one pixel and it is nearly impossible that the measurements from one station could ever perfectly match the EO estimates. The correlation values range between 0.38 and 0.49 with the slightly higher anomalies. Winter correlations show very similar pattern as for Hoal network, indicating that the data measured in winter months is in most cases not suitable for comparison and therefore after masking out very few observation remained for comparison. The S1ASCAT data provides the highest R_p in autumn, up to 0.58 and relatively low correlations in summer, which are expected to occur due to low penetration capability through growing vegetation. As the consequence of averaging of different models, it is expected that the ensemble show higher correlation than individual products.

Time	Type	Ensemble		METEO		HYDRO		AGRO		S1ASCAT	
		Rp	uRMSD	Rp	uRMSD	Rp	uRMSD	Rp	uRMSD	Rp	uRMSD
Full time	Abs.	0,438	0,050	0,401	0,052			0,377	0,053	0,490	0,045
series	Ano.	0,555	0,022	0,447	0,027			0,422	0,024	0,443	0,019
Winter	Abs.	0,206	0,028	0,405	0,016			0,413	0,015	0,406	0,035
(DJF)	Ano.	0,232	0,026	0,368	0,022			0,183	0,016	0,204	0,020
Spring	Abs.	0,383	0,045	0,241	0,045			0,300	0,040	0,380	0,047
(MAM)	Ano.	0,590	0,020	0,250	0,027			0,401	0,022	0,502	0,016
Summer	Abs.	0,364	0,047	0,186	0,056			0,226	0,054	0,394	0,045
(JJA)	Ano.	0,500	0,023	0,367	0,033			0,372	0,028	0,358	0,021
Autumn	Abs.	0,625	0,037	0,619	0,040			0,675	0,034	0,580	0,038
(SON)	Ano.	0,613	0,021	0,632	0,021			0,672	0,018	0,542	0,019

(HYDRO column: No RZSM data available from HYDRO)

Table 6.3: Validation metrics of 500m products compared to WegenerNet SM network (RZSM)

However, the R_p of ensemble (raw time series) is slightly below the R_p of S1ASCAT product but to some extent higher in comparison to two other models. Due to very few in situ datasets, it is likely to expect that averaged uRMSD estimate can be driven by some outliers, which showed in most cases to exceed the target accuracy $(0.04m^3m^{-3})$.

6.1.3 BMNT

The third SM in situ network that contributed in the final analysis is BMNT, containing stations spread across different land cover types in the country. Although in total 21 stations are installed, in this analysis the datasets of 12 stations which showed temporal and spatial matching with other four SM products were used. As the AGRO data is representing the SM data from agricultural fields it can occur that some stations have no matching data with AGRO data. Nevertheless the low number the stations, this network allows more robust spatial analysis. As mentioned before, the HYDRO model provided data only for Hoal agricultural catchment and is excluded here. Ten of 12 stations are installed in agricultural fields and one in meadow and one in forest with a very diverse elevation (3.3).

The results of validation metrics for 12 stations are reported in Table 6.4. Comparing the correlations of individual products (raw time series) it is evident that the R_p of S1ASCAT product gives considerably lower values than the other models. For instance, AGRO model shows the best correlations with in situ estimates but this model has mainly data over agricultural fields which are in flat lands in contrast to S1ASCAT which has an advantage to get retrievals over difficult areas as mountain slopes as well as over flat lands. Moreover, for the in situ station installed in forest it is very hard to retrieve SM with S1ASCAT due to very dense vegetation. This implies that the ensemble product was most likely affected by slightly inaccurate S1ASCAT SM estimates and therefore slightly lower correlations in comparison to METEO and AGRO model products can be observed, with the R_p of 0.59. The scores of anomalies range between 0.4 to 0.66 which could be interpreted that the consistent seasonality pattern occurred as well as with raw time series. The seasonal correlations of ensemble are appreciably higher than of S1ASCAT product except for winter season because lot of measurements were masked out, where the similar behavior as in the comparison with other SM networks can be found. The uRMSD are in almost all cases in the range of commonly used threshold $(0.04m^3m^{-3})$. It is recognised that the overall response of ensemble product to the changes of SM shows good agreement with Pearson correlation of 0.65 compared to in situ measurements.

Time	Type	Ensemble		METEO		HYDRO		AGRO		S1ASCAT	
		Rp	uRMSD	Rp	uRMSD	Rp	uRMSD	Rp	uRMSD	Rp	uRMSD
Full time	Abs.	0,649	0,035	0,670	0,034			0,733	0,031	0,184	0,053
series	Ano.	0,679	0,019	0,613	0,021			0,658	0,019	0,392	0,024
Winter	Abs.	-0,040	0,027	0,502	0,025			0,262	0,030	-0,005	0,032
(DJF)	Ano.	-0,033	0,021	0,530	0,020			-0,380	0,012	0,067	0,016
Spring	Abs.	0,754	0,026	0,698	0,028			0,659	0,038	0,086	0,052
(MAM)	Ano.	0,658	0,019	0,620	0,020			0,653	0,018	0,249	0,025
Summer	Abs.	0,788	0,032	0,711	0,036			0,661	0,049	0,532	0,037
(JJA)	Ano.	0,670	0,022	0,595	0,025			0,624	0,024	0,399	0,025
Autumn	Abs.	0,559	0,030	0,699	0,025			0,700	0,025	0,393	0,034
(SON)	Ano.	0,727	0,017	0,745	0,017			0,752	0,015	0,465	0,021

(HYDRO column: No RZSM data available from HYDRO)

Table 6.4: Validation metrics of 500m products compared to BMNT SM network (RZSM)

6.1.4 Ensemble validation

Second part of evaluation is related to the SM dataset downscaled to 100 m spatial resolution. The results of the comparison between ensemble and all in situ SM networks in terms of uRMSD and R_p values are reported in Table 6.5. It it evident that the values are as high as obtained of the validation analysis for 500 m products. Once again, this fact proves the assumption from the beginning that it is possible to obtain reliable SM estimates at high resolution by combining EO data with different models.

Time	In situ	Type	Ensemble - 500 m		Ensemble - 100 m	
			Rp	uRMSD	Rp	uRMSD
Full time series	Hoal	Abs.	0,676	0,042	0,662	0,030
		Ano.	0,493	0,024	0,354	0,016
	Wegenernet	Abs.	0,435	0,039	0,448	0,049
		Ano.	0,552	0,018	0,478	0,024
	BMNT	Abs.	0,589	0,040	0,419	0,044
		Ano.	0,637	0,021	0,625	0,022

Table 6.5: Validation metrics of 100m products (RZSM)

Scatterplots between the ensemble at the 100 m spatial resolution and reference datasets (SSM and RZSM) of Hoal SM network are presented in Figure 6.5, with a color coding for the different seasons. The good agreement between the two datasets is visible. However, there seems to be tendency of the ensemble product to overestimate SM in autumn.
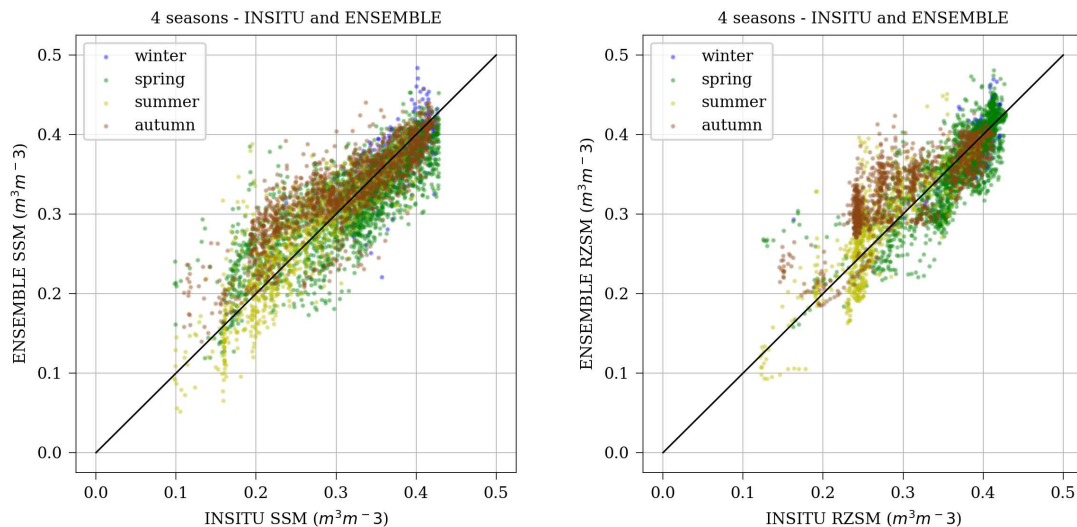
Figure 6.5: Scatterplots of ensemble and all in situ Hoal stations. SSM (left) and RZSM (right).

6.2 Groundwater comparison

An additional test of the ensemble product is carried out by comparing ensemble SM estimates with groundwater measurements. The analysis was conducted using standardized non-linear validation metric (Spearman) as well as several other metrics as autocorrelation and standard deviation of differences in order to understand and explain better the results of evaluation. In addition, the comparison with the soil porosity values and variety in land cover types will give us a better understanding of its behaviour. After the temporal and spatial matching of the ensemble grid pixel with the groundwater station, the validation scores of the comparison between them were calculated.

Figure 6.6 demonstrates the raw time series and anomalies of ensemble product and groundwater station. This groundwater station is installed in a agricultural field in Aich in Styria at the surface elevation of 694 m. As the average groundwater layer depth of this station is 2.1 m, it can be assumed that the groundwater table of this station changes very quickly so it may be well comparable to the SM variations. It is evident that the raw time series of this groundwater station are in good agreement with the ensemble. The effect of much wetter 2016 can be seen in late summer, and good response on precipitation events is fulfilled in every year. By comparing Figures 6.6 and 6.7 it can be observed how the groundwater observations response differently on the precipitation events.

Figure 6.7 represents the example of the station that is measuring groundwater layer on the averaged depth of 35.4 m. This groundwater station is installed in a grass lawn near Aichdorf in Styria at the 701 m above sea level. Its data show an relatively smooth curve with the delayed response to the rainfall events. This can be explained by the fact that rainfall takes a while before it infiltrates to deeper groundwater levels. Therefore, it may be reasonable to assume that by smoothing the SM data it becomes more comparable to groundwater measurements (Fig. 6.7). This figure also proved our hypothesis of the expected lags in the deeper groundwater
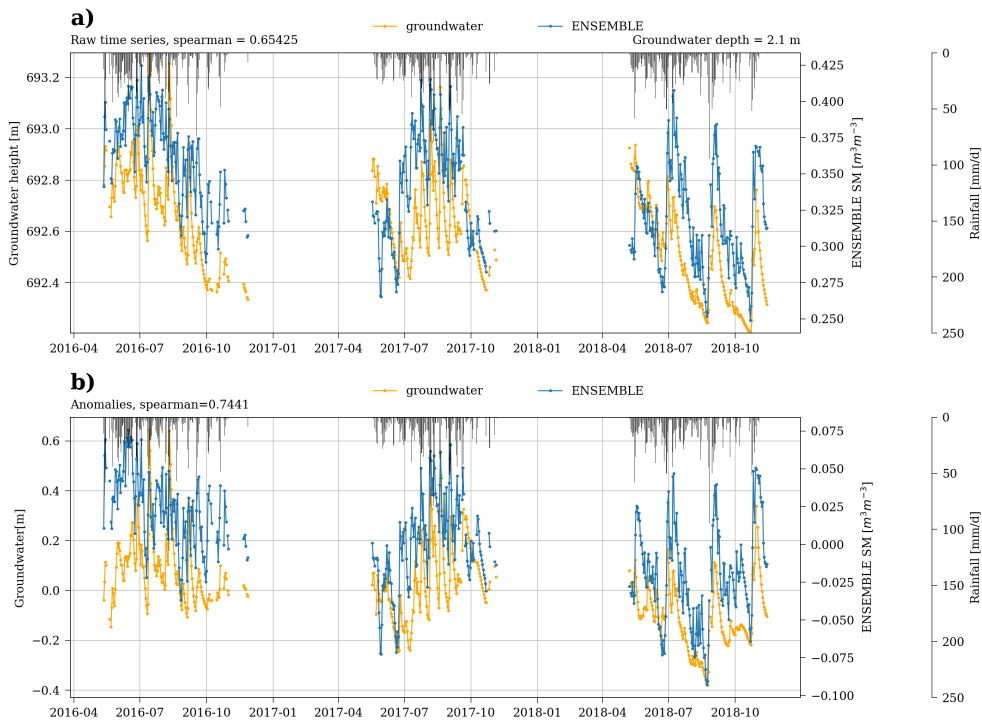
Figure 6.6: Example of a) raw and b) anomaly time series of ENSEMBLE and groundwater station at low layer depth - 2.1 m. In addition, rainfall measurements are displayed.
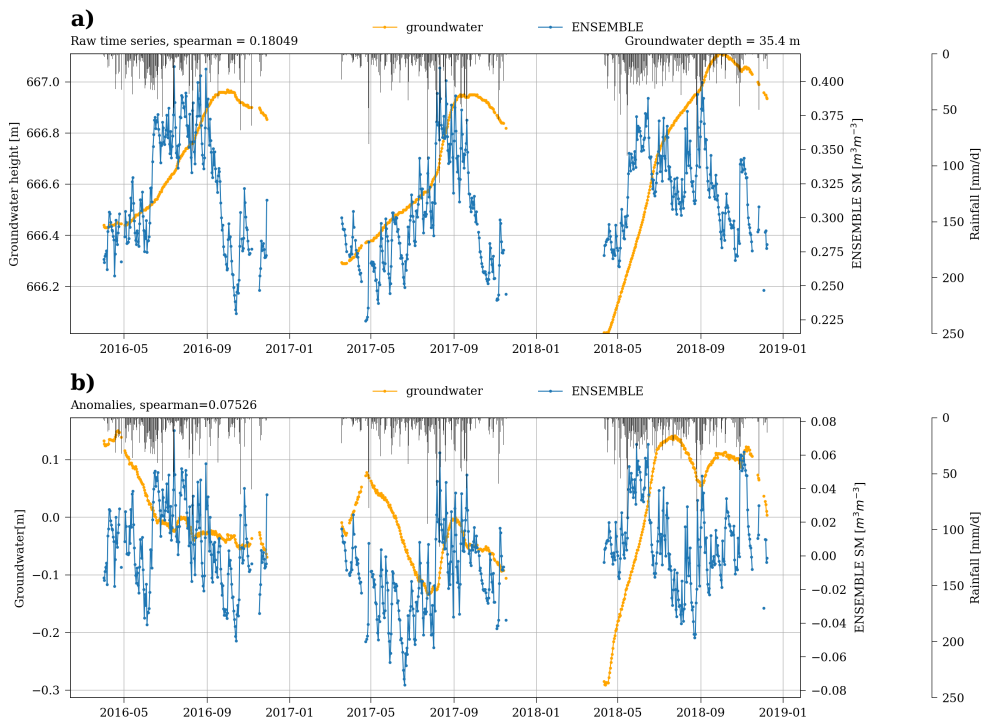
Figure 6.7: Example of a) raw and b) anomaly time series of ENSEMBLE and groundwater station at high layer depth - 35.4 m. In addition, rainfall measurements are displayed.

layers. Apparently, the groundwater in 2016 and 2018 became 2-3 months delayed response to rainfall events than in 2017, which shows an quite good agreement at the beginning of autumn in comparison to the ensemble SM estimates, where also in autumn a lag is present. In terms of R, the station that is measuring groundwater layer at small depths shows fairly high correlation, up to 0.62 with slightly higher anomalies in comparison to the correlation of -0.02 for raw time series and -0.05 for anomalies of the deeper groundwater station.

The evidence of high correlations between groundwater and SM measurements is visible in Figure 6.8, where the highest values are up to 0.87. The most R_s values are around 0.7 which implies a very good relation between SM variations and changes in groundwater level. The spatial distribution of the Spearman correlations can be observed in Figure 6.9 (Legend as in Fig. 3.4). The low correlations can be mainly found in the urban areas, around the mountains, over the needle forest or next to the water surfaces. For instance, on the region of the biggest cities (Vienna, Linz, Wiener Neustadt) lower correlation are recorded than in the east and south-east regions, where the correlations above 0.7 can be identified.
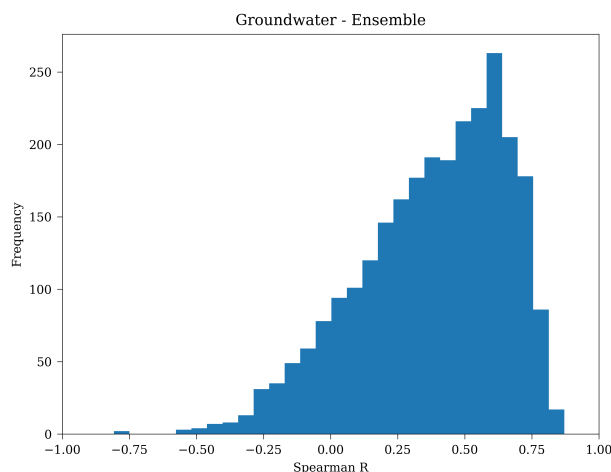
Figure 6.8: Histogram of Spearman correlation coefficient
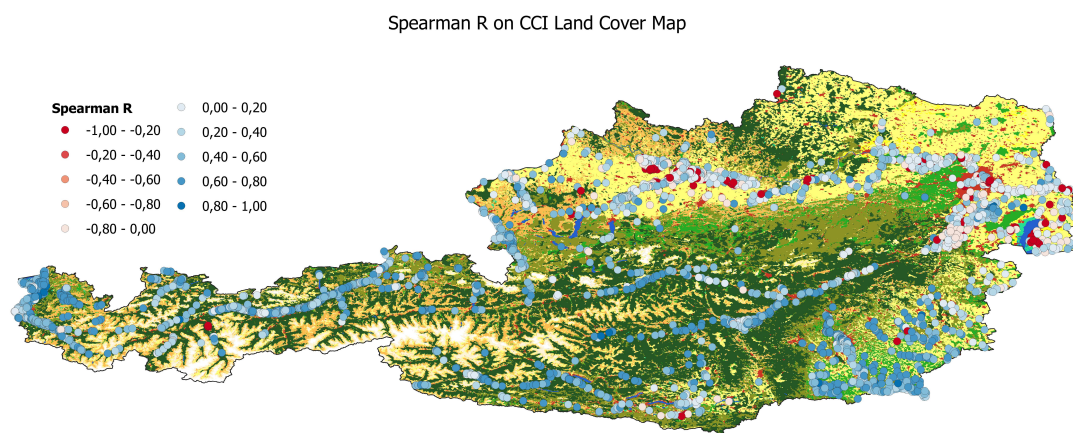
Figure 6.9: Spearman correlations between groundwater and ensemble datasets.

6.2.1 Effect of groundwater depth

Next steps in the groundwater comparison are focused on finding the relations between groundwater layer depth and several different parameters. The Figure 6.10 reveals the result of comparing groundwater layer depth in respect to the Spearman correlation coefficients. This outcome is excellent and it strongly confirms our prediction: the shallower the groundwater layer depth is, the higher correlations were calculated. It should, however, be noted that from a certain groundwater layer depth, barely no correlation can be detected. This is most likely associated to soil compaction which is one of the significant effects on the groundwater response.
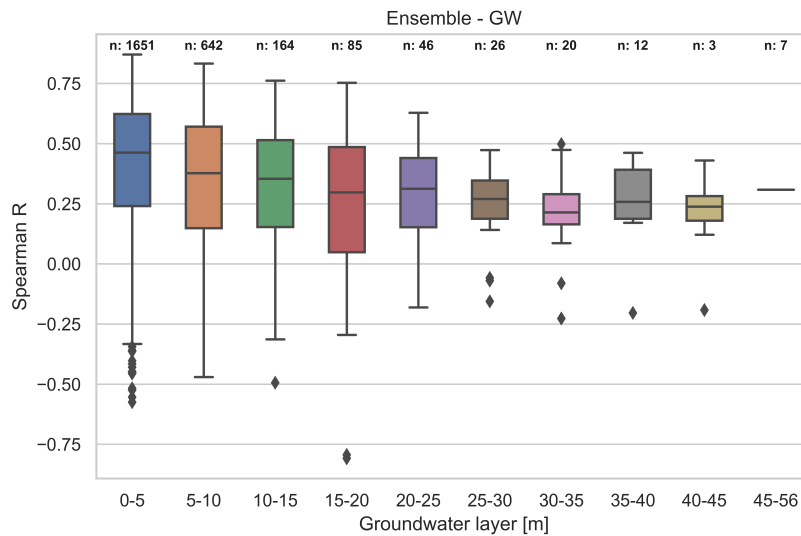
Figure 6.10: Spearman correlations in respect to groundwater layer depth, In addition, the number of stations per box is displayed.
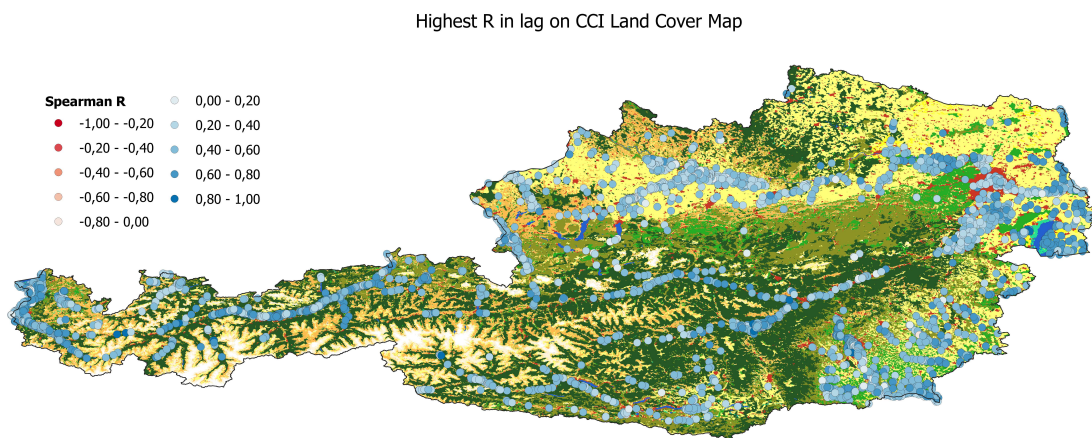
Figure 6.11: Highest spearman correlations in the lags between groundwater and ensemble datasets

Plotting the highest Spearman R correlation depending on the lag (6.11) provided a significantly better outcome in terms of higher correlations when the time shift is
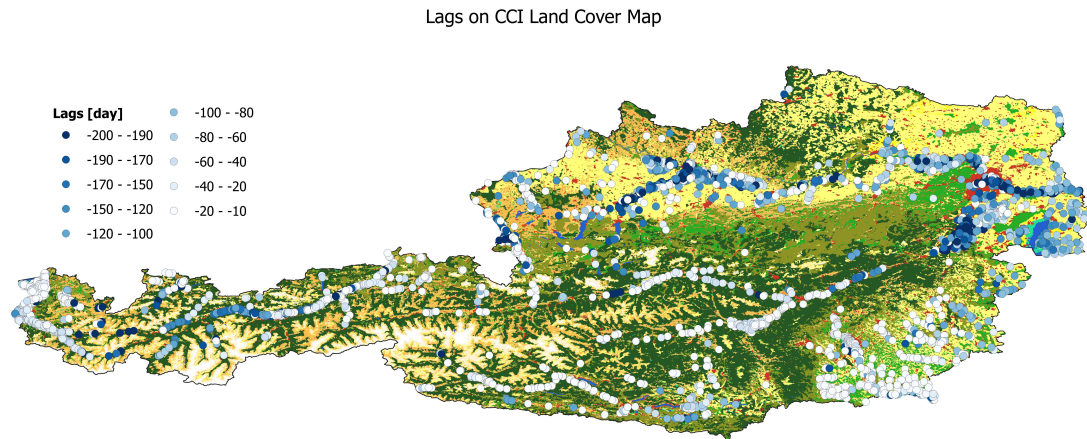
Figure 6.12: Lags in days between groundwater and ensemble datasets

applied. Hence, several influence factors as land cover types must be considered in this comparison in order to be able to offer adequate conclusions.

Figure 6.12 illustrates the lags in days, when the highest correlation have been calculated. This map should be interpreted with the Figure 6.16 as the both contain the information about the lags. In most cases, we can clearly observe that the correlations in the grassland and cropland at the shallower groundwater layer depths provide particularly high correlation in contrast to the ones that have longer delay to record SM variations. The groundwater stations that have longer delay to register changes in SM are mainly installed in needle forest, urban areas, in mountain ranges and next to the water surfaces. The longest delay is measured at the stations placed next to the rivers and in urban areas. The groundwater close to the river can be strongly affected by river level and in urban areas by having very little vegetation regions where the rain could infiltrate into the soil.

The relationship between autocorrelation of groundwater measurements and Spearman correlations can be seen in Figure (6.13). It may be recognized that the autocorrelation values are in all cases positive which indicates, as expected, the effect of existing lags in response of the groundwater. Moreover, the lower Spearman correlation coefficients were estimated at the stations that have high autocorrelation due to its very smooth behaviour caused by the time delay of water infiltration to capture changes in SM content. The highest Spearman correlations are found where the autocorrelation ranges between 0.4-0.8 which is likely to be associated to the shallower groundwater stations, which are more sensitive the capture SM variations and, therefore, their time series show slightly different course.

Next analysis compares the autocorrelation values of groundwater to depth. Expected trend of relation between the lower correlations and the shallower groundwater depth is illustrated in Figure 6.14a. Driven by the precipitation events, the higher fluctuation occurred in the upper soil level affecting the SM content. Due to the inability of deeper groundwater to reflect very small SM changes in the topsoil, a smooth behaviour of groundwater observations can be seen at the deeper groundwater depths. On the other hand, the shallower groundwater reflects better the SM variations. Therefore, the lower autocorrelation values are found in shallower groundwater which are driven by quick changes in the groundwater table. This trend will probably not be recorded from certain soil depths as it is hardly possible
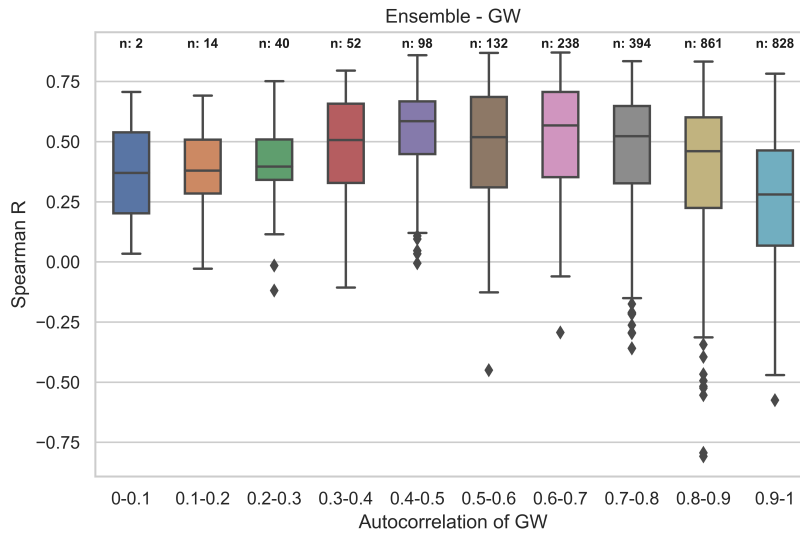
Figure 6.13: Spearman correlations in respect to autoccorelation of groundwater. In addition, the number of stations per box is displayed.

that the water infiltrates so fast and deep into the soil. To conclude, the higher the autocorrelation the lower the Spearman correlation coefficient and also the deeper groundwater level.

The values of standard deviation of differences in respect to groundwater layer depth (Fig. 6.14b) provided the similar trend as with autocorrelation values. The higher value of this estimate the better response of groundwater station to rainfall events. Even though the number of suspected outliers for the shallower groundwater layer depth is large, a tendency of fast responses is found at great number of observations of the shallower groundwater. For the deeper layer depths with the smoother behaviour of time series, the negligible response in respect to SM variations can be observed.
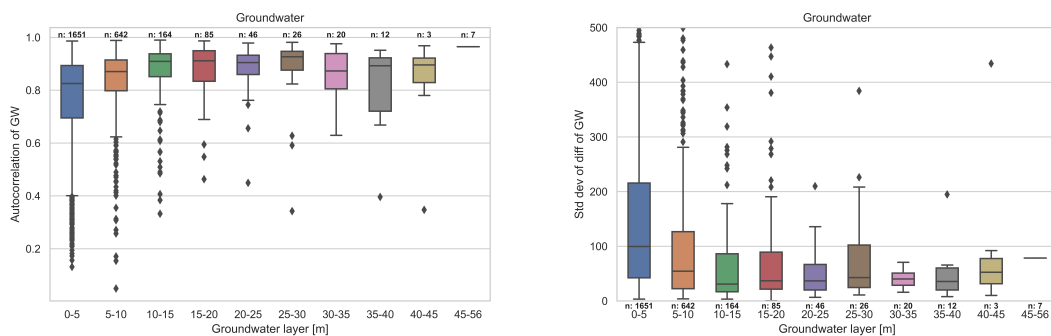
(a) Autocorrelation - GW layer depth

(b) Std dev of diff - GW layer depth

Figure 6.14: (a) Autocorrelation of GW in respect to groundwater layer depth. (b) Standard deviation of differences in respect to groundwater layer depth. In addition, the number of stations per box is displayed in both Figures.

In order to be able to investigate the correlation between the shift and the smoothness of the groundwater curve, it was necessary to investigate the relation

between the groundwater layer depth and the lags where the highest Spearman correlation coefficient was quantified. According to the Figures 6.15 and 6.16, the tendency can be seen that larger shifts lead to the highest correlations with greater depths. For instance, the correlation coefficients for the shallower groundwater do not improve a lot whereas the significant improvement can be seen in the deeper groundwater level. Therefore, by shifting the groundwater time series Spearman correlations do not vary a lot for stations with groundwater layer at 0-5 m beneath the soil surface but the changes are visible for deep layers. It may be recognized that the lag is increasing with the deeper groundwater layer. However, not only the depth of the groundwater plays a role in a shifted behaviour, but also the condition of the soil between the ground surface and the groundwater. Consequently, whether the station is measuring the changes in groundwater table in the particularly permeable or particularly impermeable layers of soil (soil compaction).
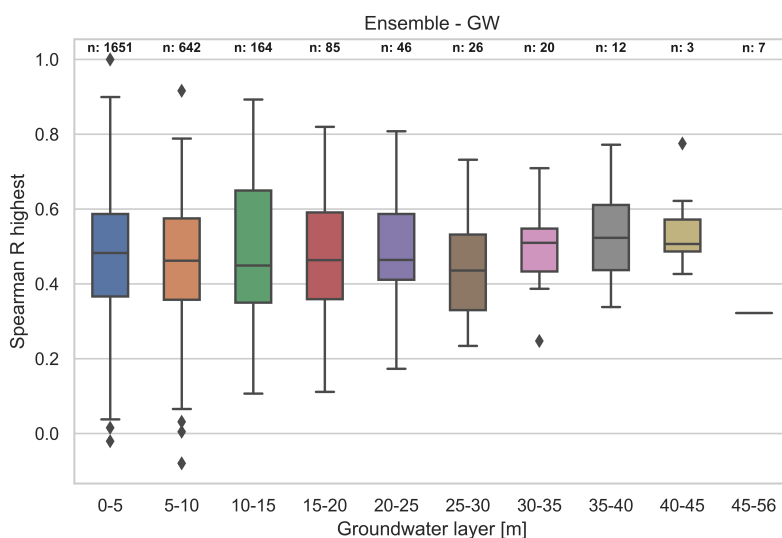
Figure 6.15: The highest spearman correlations after applying a time shift. In addition, the number of stations per box is displayed.

Figure (6.17) illustrates the result of comparison between the Spearman correlation coefficients of ensemble and groundwater time series with values of standard deviation of differences of groundwater dataset. The sensitivity of groundwater observations to capture small variations in SM is visible, the higher the correlations the higher the standard deviation of differences. The concordance scores between the correlations under 0.45 for the most stations and values of standard deviation of differences strongly confirm previous prediction of the delay time of the groundwater response to the SM variations: the higher the lag the deeper the groundwater. In conclusion, the higher the standard deviation of differences the shallower the groundwater and the lower the autocorrelation values.
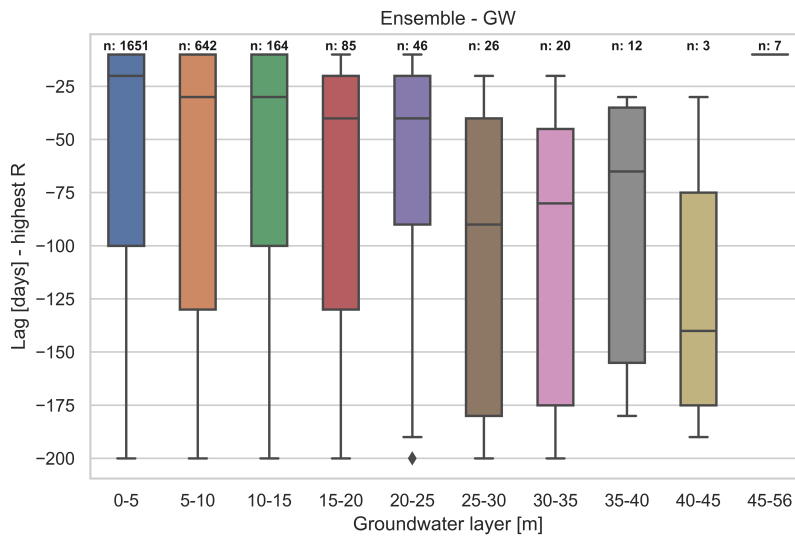
Figure 6.16: Shifts in days where highest R in respect to groundwater layer depth
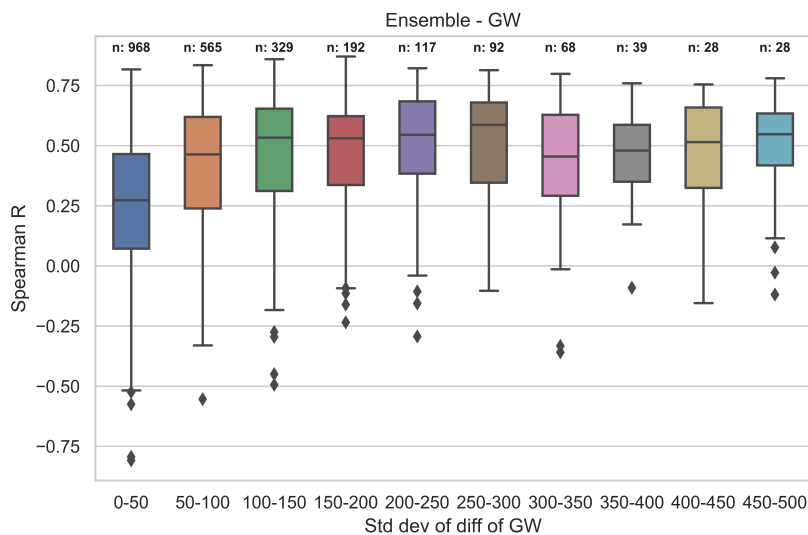
Figure 6.17: Spearman correlations in respect to standard deviation of differences. In addition, the number of stations per box is displayed.

6.2.2 Effect of soil properties

One part of spatial analysis was investigated by comparing Spearman correlation coefficients of the original data to, on one hand porosity values, and on the other hand land cover types. As the porosity represents percentage of void space in the soil, it can be proportional related to hydraulic conductivity, which describes the pace with which the water can move through pore spaces. In this case it means, the better soil infiltrates the water the better response can be observed from groundwater layer. Figure 6.18 represents the relation between porosity values and Spearman correlations, where is expected to observe that higher porosity values lead to slightly higher correlation. Slightly disappointing, here is no clear relation visible.
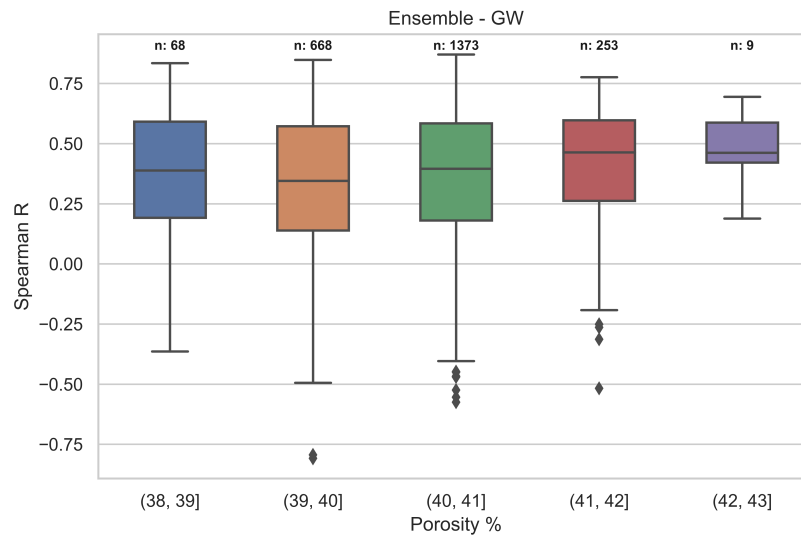
Figure 6.18: Spearman correlations in respect to porosity values

6.2.3   Effect of land cover

The effect of land cover types on the correlations between groundwater measurements and SM observations is displayed in Figure 6.19. It may be recognized that the stations installed on cropland or grassland show higher correlation than the ones that are distributed in other land cover types. Besides stations in cropland and grassland, the stations in needle forest revealed also high correlations, up to 0.6. However, in comparison to other two land types, very little stations (47) contributed to this final result. The lowest correlations are calculated in sparse indicating that these stations are most likely installed in mountainous regions or in urban areas.
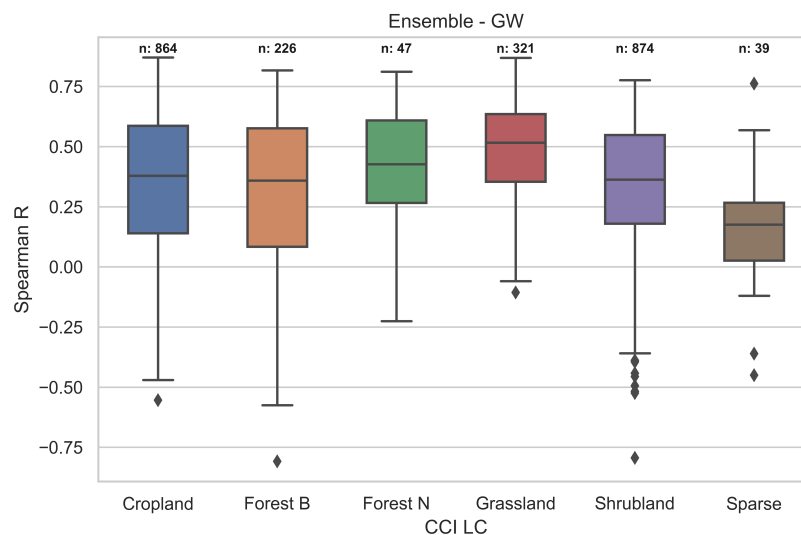
Figure 6.19: Spearman correlations in respect to land cover type

Chapter 7

Discussion

7.1   In situ soil moisture validation

Previous work has documented the importance of and need for high resolution SM EO data for improving SM monitoring at a global scale and reducing spatial errors when comparing in situ measurements with SM estimates at wide satellite footprint. Luca Brocca, Hasenauer, et al. 2011, for example, report that the discrepancies in comparison of satellite products to the in situ measurements can be related to the non-representativeness of in situ observation at the satellite pixel scale. However, these studies have used the satellite products with a low spatial resolution of several km to several dozen of km without masking out for weather conditions. In this study the capability of four high resolution SM products was tested, with the emphasis on the combined product ensemble, to retrieve reliable SM estimates. The ensemble product is a combination of four SM datasets, downscaled at the high spatial resolution of 500 m and 100 m. Moreover, it is important to assess plausibility of in situ observation, as they are used as control for S1ASCAT, model data and ensemble product.

Validation of in situ SM measurements in previous studies (Crow et al. 2012, Montzka et al. 2017) indicates that the low resolution of satellite products and up-scaling methods play an significant role when the accuracy of SM satellite data is needed. Masking out the measurements that were affected by frozen conditions is a necessary step to apply when the improvement of the quality of satellite products is sought. The second pre-processing step was related to scaling the four datasets (S1ASCAT, ensemble and three model) to the reference dataset (in situ) which could caused some additional discrepancies in the final comparison. In this work, the analysis of SM indicates that, in the analysed three study areas, in general high correlations between in situ SM measurements and product datasets were found. More specifically, in terms of Pearson correlation coefficient, as expected, the considerably high correlation of 0.71 were calculated when comparing raw time series of ensemble product and Hoal SM network at SSM layer. Validating the Hoal and BMNT SM network against AGRO model showed relatively high correlations above 0.67 which can be explained that AGRO data is captured only over agricultural fields in flat lands. Therefore, this model might seem to retrieve more reliable estimates than the S1ASCAT dataset which is, on the other hand, capable to retrieve data not only over flat lands but also over difficult areas. As the BMNT stations are installed in very diverse land cover, including mountain areas and forest, the

lower correlations of 0.2 were found between S1ASCAT dataset and BMNT SM network. The comparison with the WegenerNet SM network revealed slightly lower correlation under 0.5 in almost all cases which might be caused by low number of stations and not very reliable sensors. The ensemble product, as first of its kind, reveals improved estimates compared to the ones from S1ASCAT and three model datasets. By comparing with ensemble product, the considerably high correlations above 0.65 for Hoal and BMNT SM network were estimated and for WegenerNet SM network slightly lower up to 0.44. Additionally, by calculating the Pearson correlations and uRMSD of four seasons the good agreement between ensemble and in situ measurements was observed, with the slight overestimation SM in autumn. It must be noted, that denser and better distributed SM network should be set up in order to acquire more accurate and reliable SM estimates.

Finally, in order to generalize the result of comparison of ensemble, S1ASCAT and model datasets with in situ SM estimates, the land use characteristics of the Hoal network have been analysed more carefully. Robert Parinussa, Meesters, et al. 2011 reported the high connection between the accuracy of retrieved SM estimates from satellites and vegetation density. Theoretically, as the vegetation density increases, the observed soil emission decreases and consequently the SM information observed from microwave signal decreases. This impact is present when comparing S1ASCAT, ensemble and three model datasets with BMNT SM network as some stations are placed in forest or mountains, as well as for Hoal SM network where few stations are installed in forest area. Interestingly, the correlations between SSM and RZSM layer for the Hoal SM network does not show any big difference indicating that the SM estimates from S1ASCAT, ensemble and model datasets are in similar accuracy range captured as for SSM layer as for RZSM layer.

7.2   Groundwater validation

This study compares well with the study from Netherlands (Richard de Jeu n.d.) by using the novel approach to validate high resolution SM estimates (ensemble) with groundwater observations. The results of relatively high correlations up to 0.87 between ensemble estimates (RZSM) and groundwater observations are significantly high in comparison with previous research studies (Dorigo et al. 2015, Holgate et al. 2016), and they suggest that this approach appears to be efficient in analysing the accuracy of SM estimates. The groundwater analysis in this study proposes more wider perspective in terms of considering different kinds of external influences on the comparison of ensemble product in respect to groundwater estimates. However, some limitations are worth noting. The contrast between the ground-based groundwater sites, which represent the result of larger area contributing to groundwater layer, and the ground resolution of ensemble product (500 m) used to retrieve SM estimates represents a significant challenge for the proper validation analysis and describing their driving influences. Several effects as groundwater layer depth, soil porosity, land cover type and precipitation rate are some of the effects that are directly affecting the response of groundwater. They are highly related to each other and can not be evaluated separately. For instance, the response of the groundwater to the precipitation events is highly related to the groundwater layer depth. If infiltration rate is very high and the groundwater is quite near to the surface than very good response on rainfall events is observed and therefore good agreement with ensemble

SM estimates. The signal from the deep groundwater is very smooth due to long infiltration rate which is most likely caused by the different soil types in Austria. The result showed that the lag is increasing with the deeper groundwater which is extended by calculating the highest Spearman correlation coefficient of the lags. The correlations for the shallower groundwater do not improve a lot whereas a significant improvement is visible in the deeper groundwater level. This confirms the fact that by shifting the groundwater the higher correlations are calculated for deeper groundwater layer while the same correlations remain for shallower groundwater. The results of autocorrelation and standard deviation of differences provide more insights into the behaviour of groundwater: the higher the autocorrelation the deeper the groundwater, revealing the existing lag in the response of groundwater, and the higher the standard deviation of differences the shallower the water, proving the ability of shallower groundwater to capture small changes in SM content.

It is important to mention that one of the reasons that could be leading to the differences is that in some groundwater stations it can occur that groundwater measurements represent much larger area, as the groundwater flows from different areas to the certain point where the measuring station is located, whereas the satellite SM estimate is representing more or less the pixel measurement which is than directly compared to the groundwater observation. On the other hand, the groundwater levels can also partly be influenced by any human activities such as building dams, water pumps, reservoirs or similar human creations.

Compared to land cover types (6.9), it is evident that the low correlations were obtained in urban areas, in needle forests, close to the water surfaces and in the mountain ranges. This can be explained as follows: needle forests grow on specific type of soil which is not very deep but very rocky, indicating that the water probably takes very long until it reaches the station, and therefore, S1ASCAT has a limitation to retrieve SM estimates over dense vegetation, especially over dense forest. Urban areas are mainly covered with buildings, or road surfaces which totally disable penetration of the satellite observations. It is hard to retrieve SM estimates in mountain ranges because of the steep terrain and a lot of effects on incidence angles. Lastly, when retrieving SM from microwave observations, all water areas with a buffer of few km around them should be masked out as they are not representing the SM variations but have very high impact on the signal. On the other hand, the groundwater is probably affected when it is flowing close to the water bodies so it is assumed to cause two-way effect. The groundwater validation method applied in this work broadens the current state and expand prior research. To sum up, the overall agreement of the groundwater table to the variation in SM is excellent and encouraging and should be validated in other regions outside of Austria.

Chapter 8

Conclusion

In this study the evaluation of four SM datasets and the ensemble product, computed the average of these four SM datasets was carried out. For the evaluation the in situ measurements of 47 sites were used, which are distributed through three SM networks in Austria. As novel approach, the 2670 groundwater stations contributed to the final validation. More specifically, this work assessed the ability of the new derived ensemble product to obtain reliable high resolution SM estimates. The results of Pearson correlation coefficient and uRMSD demonstrate that the good agreement can be found when comparing ensemble product downscaled at two spatial resolutions (100m and 500 m) in respect to in situ measurements. It needs to be emphasised that the validation for Hoal SM network was applied at two depths, SSM (0-5 cm) and RZSM (20cm) and for two other SM networks (BMNT and WegenerNet) at RZSM. No big difference in correlations has been recorded between these two depth at Hoal SM network which means that the S1ASCAT, ensemble and three model datasets are able to capture well SM variations at both soil depths. Lower correlations are estimated by comparing with WegenerNet SM network as only four stations were used in this analysis. Due to the very diverse land cover types of the BMNT stations the lower correlations than for Hoal SM network were calculated, especially for S1ASCAT dataset because it is hard to retrieve SM estimates in mountain ranges due to the steep terrain and also many effects on incidence angles of satellite signal. The ensemble product captured very good precipitation events but it is likely that the high vegetation density disturb the satellite retrieval in summer months. Future studies should include more in situ stations covering different land cover types in order to be able to validate more robust analysis.

In this study the method for evaluating ensemble as high resolution SM product with the groundwater observations was proposed. The analysis was carried out by calculating standard validation metrics (Spearman), autocorrelation and standard deviation of differences combined with additional investigation of effects of land cover types and porosity throughout the country. It is apparent that several parameters in complex interrelation are driving the quality of high resolution SM products. In general, the valuable relation can be found between groundwater table and precipitation level. Moreover, the groundwater near to the surface follows very similar curse as the SM, indicating high relation between them. Very deep groundwater shows smooth behavior which can be explained due to longer time delay before the water reaches the sensor. Therefore, by smoothing the ensemble data it resulted that the delayed response, measured in lags, is highly compatible with groundwater

layer depth, indicating the deeper the groundwater layer the larger the shift. In addition, calculating the highest correlation coefficient of the lag showed improved correlations in deeper groundwater layer which is another prove of existing delay time of groundwater response to variations in SM. Another important result that contributed to the final analysis are estimates of autocorrelation and standard deviation of differences. The higher the autocorrelation the deeper the groundwater, revealing the existing lag in the response of groundwater, and, on the other hand, the higher the standard deviation of differences the shallower the water, where the assumption of the ability of shallower groundwater to capture small SM variations is confirmed. Some limitations that were encountered is this research are comparison of pixel-scale measurement of ensemble with groundwater observation which represents a measure of the catchment (larger area), than the effects of land cover types as vegetation density which reduce penetration rate of satellite signal or water surfaces which affect both the height of groundwater table and the satellite signal and lastly, the soil porosity due to the soil compaction which directly influences the water infiltration through the soil.

To sum up, this work demonstrated that, the combined product ensemble provides good agreement with in situ measurements at both depths, SSM and RZSM. When validating groundwater observations with high resolution SM estimates from ensemble, shallower groundwater measurements showed remarkable good agreement. These results fulfill the objective of the present research: it is possible to retrieve reliable high resolution SM estimates by combining EO and model data. Moreover, the existing lag in response of deeper groundwater is proved by several metrics. The groundwater observations generally have better spatial support than in situ SM sensors. The findings in this research are promising and should be explored with other groundwater networks. This study also provides the framework for future studies to assess the performance of high resolution S1ASCAT and model data in comparison to in situ measurements. An important question for future studies is to determine in detail the effects of soil porosity and heterogeneity in land cover types as on SM as well as on groundwater. In future, it is also advised to explore the influence of human activities on groundwater level as building dams, water pumps or reservoirs.

Bibliography

Albergel, Clement et al. (Feb. 2009). "An evaluation of ASCAT surface soil moisture products with in-situ observations in Southwestern France". In: *Hydrology and Earth System Sciences* 5. DOI: 10.5194/hessd-5-2221-2008.

Altman, Douglas G and J Martin Bland (2005). "Standard deviations and standard errors". In: *BMJ* 331.7521, p. 903. ISSN: 0959-8138. DOI: 10.1136/bmj.331.7521.903. eprint: https://www.bmj.com/content/331/7521/903.full.pdf. URL: https://www.bmj.com/content/331/7521/903.

Blöschl, G. et al. (Jan. 2016). "The Hydrological Open Air Laboratory (HOAL) in Petzenkirchen: A hypothesis-driven observatory". In: *Hydrology and Earth System Sciences* 20, pp. 227–255. DOI: 10.5194/hess-20-227-2016.

Brocca, Luca, Stefan Hasenauer, et al. (Jan. 2011). "Soil moisture estimation through ASCAT and AMSR-E sensors: An intercomparison and validation study across Europe". In: *Remote Sensing of Environment* 115, pp. 3390–3408.

Brocca, Luca, Christian Massari, et al. (Sept. 2015). "Rainfall estimation from in situ soil moisture observations at several sites in Europe: An evaluation of the SM2RAIN algorithm". In: *Journal of Hydrology and Hydromechanics* 63, pp. 201–209. DOI: 10.1515/johh-2015-0016.

Brocca, Luca, F. Melone, et al. (Oct. 2010). "Improving runoff prediction through the assimilation of the ASCAT soil moisture product". In: *Hydrology and Earth System Sciences* 14, pp. 1881–1893. DOI: 10.5194/hess-14-1881-2010.

cek, Michael et al. (Apr. 2012). "Potential for High Resolution Systematic Global Surface Soil Moisture Retrieval via Change Detection Using Sentinel-1". In: *IEEE Journal of Selected Topics in Applied Earth Observations and Remote Sensing* 5, pp. 1303–1311. DOI: 10.1109/JSTARS.2012.2190136.

Colliander, Andreas et al. (Mar. 2017). "Validation of SMAP surface soil moisture products with core validation sites". In: *Remote Sensing of Environment* 191, pp. 215–231. DOI: 10.1016/j.rse.2017.01.021.

Crow, Wade et al. (Jan. 2012). "Up-scaling sparse ground-based soil moisture observations for the validation of coarse-resolution satellite soil moisture products". In: *Rev. Geophys* 50.

Das, Narendra et al. (Apr. 2014). "Tests of the SMAP Combined Radar and Radiometer Algorithm Using Airborne Field Campaign Observations and Simulated Data". In: *Geoscience and Remote Sensing, IEEE Transactions on* 52, pp. 2018–2028. DOI: 10.1109/TGRS.2013.2257605.

Deng, Khidir et al. (Mar. 2019). "Operational Soil Moisture from ASCAT in Support of Water Resources Management". In: *Remote Sensing* 11, p. 579. DOI: 10.3390/rs11050579.

Dorigo, WA et al. (2015). "Evaluation of the ESA CCI soil moisture product using ground-based observations". In: *Remote Sensing of Environment* 162, pp. 380–395.

Dunne, Thomas, Weihua Zhang, and Brian F Aubry (1991). "Effects of rainfall, vegetation, and microtopography on infiltration and runoff". In: *Water Resources Research* 27.9, pp. 2271–2285.

Ebert, Elizabeth (Oct. 2001). "Ability of a Poor Man's Ensemble to Predict the Probability and Distribution of Precipitation". In: *Monthly Weather Review - MON WEATHER REV* 129. DOI: `10.1175/1520-0493(2001)129<2461:AOAPMS>2.0.CO;2`.

Entekhabi, D. et al. (Aug. 2008). "Soil Moisture Active/Passive (SMAP) Mission concept". In: *Proceedings of SPIE - The International Society for Optical Engineering.* DOI: `10.1117/12.795910`.

Entekhabi, Dara et al. (June 2010). "Performance Metrics for Soil Moisture Retrievals and Application Requirements". In: *Journal of Hydrometeorology* 11. DOI: `10.1175/2010JHM1223.1`.

Figa-saldaña, J. et al. (June 2002). "The Advanced Scatterometer (ASCAT) on the Meteorological Operational (MetOp) platform: A follow on for European wind scatterometers". In: *Canadian Journal of Remote Sensing* 28. DOI: `10.5589/m02-035`.

Gruber, Alexander et al. (July 2013). "Potential of Sentinel-1 for high-resolution soil moisture monitoring". In: pp. 4030–4033. ISBN: 978-1-4799-1114-1. DOI: `10.1109/IGARSS.2013.6723717`.

Hao, Zengchao and Amir AghaKouchak (Feb. 2014). "A Nonparametric Multivariate Multi-Index Drought Monitoring Framework". In: *Journal of Hydrometeorology* 15, pp. 89–101. DOI: `10.1175/JHM-D-12-0160.1`.

Hasenauer, Stefan (Feb. 2020). "On the potential of MetOp ASCAT-derived soil wetness indices as a new aperture for hydrological monitoring and prediction: A field evaluation over Luxembourg". In: *Hydrological Processes.*

Hersbach, H et al. (2019). "Global reanalysis: goodbye ERA-Interim, hello ERA5". In: *ECMWF Newsl* 159, pp. 17–24.

Holgate, Chiara et al. (Sept. 2016). "Comparison of remotely sensed and modelled soil moisture data sets across Australia". In: *Remote Sensing of Environment* 186, pp. 479–500. DOI: `10.1016/j.rse.2016.09.015`.

Hollmann, R. et al. (Oct. 2013). "The ESA Climate Change Initiative: Satellite Data Records for Essential Climate Variables". In: *Bulletin of the American Meteorological Society* 94, pp. 1541–1552. DOI: `10.1175/BAMS-D-11-00254.1`.

Huitema, Bradley and Sean Laraway (Aug. 2006). "Autocorrelation". In:

J. Fuchsberger, G. Kirchengast (n.d.). *Deriving Soil Moisture from Matric Potential in the WegenerNet Climate Station Network.* URL: `http://www.wegenernet.org/misc/WegenerNet_TechNote-SoilMoisture.pdf`. (Accessed: 2020-03-08).

Kerr, Y.H. et al. (Sept. 2001). "Soil Moisture Retrieval from Space: The Soil Moisture and Ocean Salinity (SMOS) Mission". In: *Geoscience and Remote Sensing, IEEE Transactions on* 39, pp. 1729–1735. DOI: `10.1109/36.942551`.

Kottek, Markus et al. (May 2006). "World Map of the Köppen-Geiger Climate Classification Updated". In: *Meteorologische Zeitschrift* 15, pp. 259–263. DOI: `10.1127/0941-2948/2006/0130`.

Los, F. (Jan. 2009). "Eco-hydrodynamic modelling of primary production in coastal waters and lakes using BLOOM". In:

Martínez-Fernández, José et al. (Feb. 2016). "Satellite soil moisture for agricultural drought monitoring: Assessment of the SMOS derived Soil Water Deficit Index". In: *Remote Sensing of Environment* 177, pp. 277–286. DOI: 10.1016/j.rse.2016.02.064.

Merlin, Olivier et al. (Mar. 2013). "Self-calibrated evaporation-based disaggregation of SMOS soil moisture: An evaluation study at 3 km and 100 m resolution in Catalunya, Spain". In: *Remote Sensing of Environment* 130, pp. 25–38. DOI: 10.1016/j.rse.2012.11.008,.

Montzka, Carsten et al. (Jan. 2017). "Validation of Spaceborne and Modelled Surface Soil Moisture Products with Cosmic-Ray Neutron Probes". In: *Remote Sensing* 9, p. 103. DOI: 10.3390/rs9020103.

Parinussa, Robert, Thomas Holmes, et al. (Apr. 2015). "A Preliminary Study toward Consistent Soil Moisture from AMSR2". In: *Journal of Hydrometeorology* 16, pp. 932–947. DOI: 10.1175/JHM-D-13-0200.1.

Parinussa, Robert, A. Meesters, et al. (Aug. 2011). "Error Estimates for Near-Real-Time Satellite Soil Moisture as Derived From the Land Parameter Retrieval Model". In: *Geoscience and Remote Sensing Letters, IEEE* 8, pp. 779–783. DOI: 10.1109/LGRS.2011.2114872.

Richard de Jeu, Anne de Nijs (n.d.). *Dense groundwater networks as an unexplored evaluaton tool for satellite soil moisture.* Accessed: 2020-03-08.

Rodell, Matthew, Isabella Velicogna, and James Famiglietti (Sept. 2009). "Satellite Based Estimates of Groundwater Depletion in India". In: *Nature* 460, pp. 999–1002. DOI: 10.1038/nature08238.

Rüdiger, Christoph et al. (Oct. 2016). "Disaggregation of Low-Resolution L-Band Radiometry Using C-Band Radar Data". In: *IEEE Geoscience and Remote Sensing Letters* 13, pp. 1–5. DOI: 10.1109/LGRS.2016.2583433.

Schneeberger, K. et al. (Nov. 2004). "Topsoil Structure Influencing Soil Water Retrieval by Microwave Radiometry". In: *Vadose Zone Journal - VADOSE ZONE J* 3, pp. 1169–1179. DOI: 10.2113/3.4.1169.

Scott, Christopher, W.G.M. Bastiaanssen, and Mobin-ud-Din Ahmad (Oct. 2003). "Mapping Root Zone Soil Moisture Using Remotely Sensed Optical Imagery". In: *Journal of Irrigation and Drainage Engineering-asce - J IRRIG DRAIN ENG-ASCE* 129. DOI: 10.1061/(ASCE)0733-9437(2003)129:5(326).

Simunek Jiri, Jirka et al. (Jan. 2008). *The HYDRUS-1D Software Package for Simulating the One-Dimensional Movement of Water, Heat, and Multiple Solutes in Variably-Saturated Media.*

Soulis, Konstantinos, Stamatios Elmaloglou, and Nicholas Dercas (Jan. 2015). "Investigating the effects of soil moisture sensors positioning and accuracy on soil moisture based drip irrigation scheduling systems". In: *Agricultural Water Management* 148, pp. 258–268. DOI: 10.1016/j.agwat.2014.10.015.

Steinheimer, Martin and Thomas Haiden (Apr. 2007). "Improved nowcasting of precipitation based on convective analysis fields". In: *Advances in Geosciences* 10. DOI: 10.5194/adgeo-10-125-2007.

Wagner, W. et al. (July 2012). "Fusion of active and passive microwave observations to create an Essential Climate Variable data record for soil moisture". In: *ISPRS*

Annals of Photogrammetry, Remote Sensing and Spatial Information Sciences I-7, pp. 315–321. DOI: `10.5194/isprsannals-I-7-315-2012`.

Wagner, Wolfgang, Carsten Pathe, et al. (Feb. 2008). "Temporal Stability of Soil Moisture and Radar Backscatter Observed by the Advanced Synthetic Aperture Radar (ASAR)". In: *Sensors* 8. DOI: `10.3390/s8021174`.

Wagner, Wolfgang, Daniel Sabel, et al. (Nov. 2010). "THE POTENTIAL OF SENTINEL-1 FOR MONITORING SOIL MOISTURE WITH A HIGH SPATIAL RESOLUTION AT GLOBAL SCALE". In:

Wanders, Niko, M.F.P. Bierkens, et al. (Aug. 2014). "The benefits of using remotely sensed soil moisture in parameter identification of large-scale hydrological models". In: *Water Resources Research* 50, pp. 10215–. DOI: `10.1002/2013WR014639`.

Wanders, Niko, D. Karssenberg, et al. (June 2014). "The suitability of remotely sensed soil moisture for improving operational flood forecasting". In: *Hydrology and Earth System Sciences* 18. DOI: `10.5194/hess-18-2343-2014`.

Wang, Tiejun et al. (Feb. 2016). "Feasibility analysis of using inverse modeling for estimating natural groundwater recharge from a large-scale soil moisture monitoring network". In: *Journal of Hydrology* 533. DOI: `10.1016/j.jhydrol.2015.12.019`.